Redox Biology 59 (2023) 102547

Contents lists available at ScienceDirect

Redox Biology

journal homepage: www.elsevier.com/locate/redox

Fatty acid-binding proteins 3 and 5 are involved in the initiation of mitochondrial damage in ischemic neurons

Qingyun Guo [a,b], Ichiro Kawahata [b,**], An Cheng [b], Haoyang Wang [b], Wenbin Jia [b], Hiroshi Yoshino [b,c], Kohji Fukunaga [b,d,*]

[a] Key Laboratory of Brain Science Research & Transformation in Tropical Environment of Hainan Province, Hainan Medical University, Haikou, 571199, China
[b] Department of CNS Drug Innovation, Graduate School of Pharmaceutical Sciences, Tohoku University, Sendai, 980-8578, Japan
[c] Shiratori Pharmaceutical Co., Ltd., R&D Center, Narashino, 275-0016, Japan
[d] BRI Pharma Incorporated, R&D Center, Sendai, 982-0804, Japan

ARTICLE INFO

Keywords:
Ischemic stroke
Fatty acid-binding proteins
Mitochondria damage
4-HNE
BAX

ABSTRACT

We have previously shown that a fatty acid-binding protein7 (FABP7) inhibitor ameliorates cerebral ischemia-reperfusion injury in mice, suggesting an association between FABPs and ischemic neuronal injury. However, the precise role of FABPs in ischemic neuronal injury remains unclear. In this study, we investigated the role of FABPs in ischemia-reperfusion neuronal injury. FABP3, FABP5, and FABP7 were upregulated in the ischemic penumbra regions in mice. However, only FABP3 and FABP5 were expressed in injured neurons. Furthermore, FABP3 and FABP5 accumulated in the mitochondria of ischemic neurons. Overexpressing either FABP3 or FABP5 aggravated the reduced mitochondrial membrane potential and induced cell death in human neuroblastoma SH-SY5Y cells during oxidative stress. This damage was mediated by the formation of BAX-containing pores in the mitochondrial membrane. Moreover, FABP5 mediates lipid peroxidation and generates toxic by-products (i.e., 4-HNE) in SH-SY5Y cells. HY11-08 (HY08), a novel FABP3 and 5 inhibitor that does not act on FABP7, significantly reduced cerebral infarct volume and blocked FABP3/5-induced mitochondrial damage, including lipid peroxidation and BAX-related apoptotic signaling. Thus, FABP3 and FABP5 are key players in triggering mitochondrial damage in ischemic neurons. In addition, the novel FABP inhibitor, HY08, may be a potential neuroprotective treatment for ischemic stroke.

1. Introduction

Stroke is the leading cause of disability and cognitive deficits, and is the second leading cause of mortality worldwide. Approximately 80% of cases are ischemic stroke [1]. Neuronal death is a major cause of disability and death in stroke patients that occurs shortly after an ischemic episode. Owing to their inherently high energy demands, neurons are particularly susceptible to low glucose and ATP and are extremely vulnerable to ischemic events [2]. Neurons in the ischemic core area die within the first few hours, whereas cells in the surrounding ischemic penumbra suffer reversible damage that lasts for hours to days, finally leading to cell death [3]. Currently, the development of neuroprotective agents is slow and remains difficult. Thus, it is necessary to investigate specific pathways or critical molecules involved in ischemic neuronal death to develop novel ischemic stroke treatment strategies.

Mitochondria are the most important organelles for cellular energy metabolism and are critical for neuronal survival [4,5]. Although there are various pathways regulating neuronal death following cerebral ischemia, mitochondrial dysfunction is a major cause of cell death. Maintaining mitochondrial function homeostasis is crucial for neuronal survival and function. During ischemia-reperfusion, mitochondria are the main source of oxidative stress [6,7]. In mitochondria, large amounts of free radicals and reactive oxygen species are produced, which cause oxidative damage to lipids, proteins, and DNA. Lipid peroxidation is a key manifestation of the oxidative stress response from ischemia-reperfusion and is closely related to ischemic neuronal death [8,9]. Mitochondria contain abundant polyunsaturated fatty acids that are prone to lipid peroxidation. Importantly, mitochondrial membrane proteins are the main targets of lipid peroxidation-mediated damage. The major product of lipid peroxidation, 4-hydroxynonenal (4-HNE) rapidly accumulates after cerebral ischemic injury [10,11].

* Corresponding author. 6-3 Aramaki-Aoba, Aoba, Sendai, 980-8578, Japan.
** Corresponding author.
E-mail addresses: kawahata@tohoku.ac.jp (I. Kawahata), kfukunaga@tohoku.ac.jp (K. Fukunaga).

https://doi.org/10.1016/j.redox.2022.102547
Received 4 October 2022; Received in revised form 15 November 2022; Accepted 17 November 2022
Available online 26 November 2022

Abbreviations

AA	arachidonic acid
ANOVA	analysis of variance
ANS	1-anilinonapthalene 8-sulfonic acid
BBB	blood–brain barrier
BAX	Bcl-2-associated X protein
Bcl-2	B-cell lymphoma-2
CMC	carboxymethyl cellulose
FABP	fatty acid-binding protein
GST	glutathione S-transferase
4-HNE	4-hydroxynonenal; I/R, ischemia/reperfusion
MOMP	mitochondrial outer membrane permeabilization
NAC	N-Acetyl cysteine
PBS	phosphate-buffered saline
PFA	paraformaldehyde
ROS	reactive oxygen species
SEM	standard error of the mean
tMCAO/R	transient middle cerebral artery occlusion/reperfusion
T-TBS	Tris-buffered saline with 0.1% Tween 20
TTC	2,3,5-triphenyltetrazolium chloride
VDAC-1	Voltage-dependent anion-selective channel 1

Furthermore, the endogenous pathway mediating apoptosis is the mitochondrial pathway that is characterized by mitochondrial outer membrane permeabilization (MOMP) and subsequent cytochrome *c* release [12]. The pro-apoptotic protein BAX is the direct executor of MOMP. BAX is mostly found in the cytoplasm of healthy cells. However, once activated, BAX oligomerizes on the mitochondrial outer membrane, which facilitates MOMP. Then, cytochrome *c* is released into the cytoplasm, thereby initiating caspase-linked reactions that lead to cell death [13,14]. Thus, BAX oligomerization is an important element in determining the initiation of apoptosis. However, the specific mechanism of BAX oligomerization remains unclear.

FABPs are a family of lipid chaperone proteins that enhance cellular fatty acid solubilization, transport, and metabolism. These proteins are essential for lipid metabolism, gene regulation, cell signaling, and cell proliferation and differentiation. FABPs are divided into at least 12 subtypes, each with different tissue specificities. FABP3, FABP5, and FABP7 are expressed in the brain. Many studies have linked these three FABP subtypes to neuronal damage and inflammatory pathways in various neurodegenerative disorders [15–19]. Abnormal FABP expression occurs in patients with neurodegenerative diseases, such as Alzheimer's and Parkinson's disease. FABP3 levels in the cerebrospinal fluid [20] and FABP7 in the blood [21] are significantly elevated in these neurodegenerative diseases. FABP3 and FABP7 are important molecules in Parkinson's disease pathogenesis because they induce α-synuclein aggregation [22]. Furthermore, FABP5 upregulation hastens the onset of experimental autoimmune encephalomyelitis (EAE) in mice, a model of multiple sclerosis [23,24]. In amyotrophic lateral sclerosis (ALS) mouse astrocytes, FABP7 overexpression directly enhances nuclear factor-κB (NF-κB)-driven inflammatory responses and ultimately reduces motor neuron survival [25]. Although these findings suggest that FABPs may play a role in the onset and progression of neurodegenerative diseases, there have been few studies on FABP during ischemic stroke.

In a previous study, we revealed that a FABP7 inhibitor, MF6, which has high binding affinity for FABP7 but weakly binds FABP3 and FABP5, significantly rescued cerebral ischemia-reperfusion injury in mice with transient middle cerebral artery occlusion by inhibiting inflammatory-related responses [26]. This result implies that FABP7 may be involved in the development of ischemic stroke. Moreover, it remains unknown whether FABP3 and FABP5 are also linked to the development of ischemic brain injury, and whether FABPs play a direct role in ischemic neuronal death. Thus, we investigated the role of FABP3 and FABP5 in ischemic brain injury. We synthesized and screened HY11-08 (HY08), a novel ligand with a strong affinity for FABP3/5. Then, we explored the relationship between FABPs and ischemic neuronal apoptosis in cerebral ischemia-reperfusion mice to determine whether FABPs are involved in apoptosis. Our study will facilitate understanding the association between FABPs and ischemic neuronal death.

2. Materials and methods

2.1. Animals

Male ICR mice (5 weeks old, 25–30 g) were purchased from Japan SLC Inc. (Shizuoka, Japan). The animals were housed under conditions of constant temperature and humidity, with a 12-h light-dark cycle (lights on: 09:00–21:00), and *ad libitum* access to food and water. All procedures for handling animals complied with the Guide for Care and Use of Laboratory Animals and were approved by the Animal Experimentation Committee of the Tohoku University Graduate School of Pharmaceutical Sciences.

2.2. Surgical procedures used for establishing tMCAO/R

A mouse model of transient middle cerebral artery occlusion/reperfusion (tMCAO/R) was created as previously described [27]. Briefly, all mice were anesthetized with a combination of 0.3 mg/kg medetomidine, 4.0 mg/kg midazolam, and 5.0 mg/kg butorphanol. The tMCAO surgical procedure was performed as follows: a silicone-coated 6–0 suture (Doccol Corporation, USA) was inserted from the right external carotid artery to the internal carotid artery, extending to the origin of the middle cerebral artery. The suture was left in place for 2 h. Then, the suture was removed, and reperfusion was performed. Mice in the sham operation group underwent the same procedure, except the suture was not inserted. Following reperfusion, mice were sacrificed at the indicated time points. During ischemia/reperfusin (I/R), the core body temperature of each mouse was maintained at 37 °C using a homoeothermic heating blanket. Regional cerebral blood flow (rCBF) was monitored using laser Doppler flowmetry (FLOC1, OMEGAWAVE, Tokyo, Japan) to confirm whether the right brain hemisphere was in an ischemic state. Surgery was considered successful when rCBF was reduced by approximately 70–90%, as previously described [28].

2.3. Infarct volume evaluation

After 24 h or 7 days of reperfusion, the mice were decapitated, the brains were rapidly removed, and were chilled at −30 °C for 10 min. The brains were cut into five 2-mm thick slices, incubated in 1% 2,3,5-triphenyltetrazolium chloride (TTC, Wako, Japan) for 20 min at 37 °C, and soaked overnight in 4% paraformaldehyde (PFA; Sigma, USA). This procedure stained the non-infarcted parts red, whereas the infarcted areas appeared white. Infarct volumes were measured using ImageJ software (NIH, Bethesda, MA, USA) and are represented as the percentage of the total hemisphere.

2.4. Neurological score

Neurological function was evaluated prior to collecting mouse brain tissue using a neurological deficit grading system with a scale ranging from 0 to 4, as described previously [28]. The following scale was employed as a rating system: 0, normal motor function; 1, forelimb flexion when lifted by the tail; 2, circling to the contralateral side when held by the tail on a flat surface, but in a normal posture at rest; 3, spontaneous leaning towards the contralateral side when moving freely; and 4, no spontaneous motor activity with an apparent reduction in consciousness. Mice in the sham operation group exhibited no neurological deficits.

2.5. Drug administration

HY08 was provided by Shiratori Pharmaceutical Co., Ltd. The chemical structure of HY08 is shown in Fig. 2A. HY08 was dissolved in 0.5% carboxymethyl cellulose (CMC) and administered p.o. at different doses (0.05, 0.1, 0.3 or 1.0 mg/kg) immediately before the experiments were initiated, according to the experimental schedule described in Supplemental Figs. 1A and B. An equivalent volume of 0.5% CMC was orally administered to the corresponding control group.

2.6. ANS replacement assay

The affinity of HY08 for FABPs was assessed using the 1-anilinonaphthalene 8-sulfonic acid (ANS) displacement assay [29]. Briefly, N-terminal glutathione S-transferase (GST)-tagged FABPs were prepared in E. Coli BL21(DE3) competent cells (Novagen, Madison, WI, USA) and purified using GST purification kit (Clontech) as per manufacturer's protocol. 4 μM ANS, HY08 (0, 0.1, 1.0, 2.0, 4.0 μM), and 0.4 μM GST-FABP3 (or GST-FABP5 or GST-FABP7) were mixed in reaction buffer (10 mM KH_2PO_4, pH 7.5 and 40 mM KCl). After incubation for 2 min at 25 °C, the fluorescence intensity was measured at 355/460 nm using a Flex Station 3 spectrophotometer (Molecular Devices, San Jose, CA, USA). Fluorescence intensity was calculated as a percentage of it in the absence of HY08 (0 μM). The apparent dissociation constant (K_d) was analyzed by nonlinear regression using the GraphPad Prism 8 software (GraphPad Software Inc., San Diego, CA, USA). K_d values were estimated in three separate experiments. The data are presented as the mean ± SEM.

2.7. Cell culture and transfection

Human neuroblastoma cells (SH-SY5Y) were obtained from the RIKEN BRC Cell Bank (Tsukuba, Japan). Cells were cultured in Dulbecco's modified Eagle's medium (DMEM, Wako) supplemented with 15% fetal bovine serum (FBS, Gibco, CA, USA) and 1% penicillin-streptomycin at 37 °C in a humidified incubator with 5% CO_2/95% air. Human FABP3 or FABP5 expression plasmids were produced and inserted into the multiple cloning site of plasmid pcDNA3.1 (Invitrogen, Carlsbad, CA, USA). A noncoding plasmid (pcDNA3.1) was used as the control group. The human FABP5 shRNA plasmid was obtained from Sigma-Aldrich. The sequence was CCGGTGAGCAAATCTCCATACTGTTCTCGAGAACAGTATGGAGATTTGCTCATTTTTTG. Cell transfection was carried out using Lipofectamine LTX and Plus Reagent (Invitrogen) by incubation for 6 h at 37 °C. At 48 h post-transfection, cells were treated with rotenone, HY08, N-acetylcysteine (NAC), Bax inhibitor peptide V5 (BIP–V5), or BSA-fatty acid. After treatment, the cells were maintained in DMEM (1% penicillin-streptomycin) without FBS for 24 h and were then used for the following experiments. Rotenone (1 μM), HY08 (0.3 μM), NAC (1 μM), and BIP-V5 (50 μM) were prepared in dimethyl sulfoxide (DMSO). Arachidonic acid (AA), docosahexaenoic acid (DHA), linoleic acid (LA), and oleic acid (OA) were incubated with BSA (Sigma, A7030, fatty acid free) at a 1:5 ratio in binding buffer (10 mM Tris-HCl pH 8.0, 150 mM NaCl) at 37 °C for 30 min to prepare BSA-fatty acid complexes.

2.8. Mitochondria isolation

Mitochondria and cytoplasm were isolated as previously described [30]. Briefly, brain tissues or cells were suspended in mitochondrial isolation buffer (250 mM sucrose, 1 mM dithiothreitol, 10 mM KCl, 1 mM EDTA, 1.5 mM $MgCl_2$, protease inhibitors, and 20 mM Tris-HCl, pH 7.4) and were then homogenized with approximately 50 strokes of a glass-pestle homogenizer on ice. The homogenate was centrifuged three times at 800×*g* for 10 min. The supernatant was then centrifuged at 15,000×*g* for 10 min. The supernatants were collected as cytosolic fractions (without mitochondria). The mitochondrial pellets were immediately washed three times with mitochondrial isolation buffer and were subsequently homogenized with Triton X-100 buffer, as described above. The supernatants were collected as mitochondrial fractions. All steps were performed at 4 °C. Protein concentrations were determined using Bradford assays. The quantity of cytosolic fractions and mitochondria were estimated by quantifying β-actin and voltage-dependent anion channel (VDAC)-1, respectively, via Western blot assay.

2.9. Cell counting kit assay

Cell viability was measured using CCK-8 Cell Counting Kit-8 (Dojindo, Kumamoto, Japan). Cells were cultured in 96-well microplates and 10 μL of CCK-8 solution were added to each well. Plates were incubated for 2 h at 37 °C. The optical absorbance at 450 nm was measured using a microplate reader (Flex Station 3, Molecular Devices, San Jose, CA, USA).

2.10. Measurement of mitochondrial membrane potential

The mitochondrial membrane potential was measured using a JC-1 MitoMP Detection Kit (Dojindo, MT09, Kumamoto, Japan). JC-1 is a cationic fluorescent dye that forms aggregates and emits red fluorescence at high membrane potentials. However, when the membrane potential decreases, JC-1 becomes a monomer and emits green fluorescence. Cells were cultured in 35 mm glass-bottom dishes (Matsunami Glass Ind., Osaka, Japan) and treated with rotenone and HY08 (or FABP plasmid/NAC). Treated cells were incubated with 2 μM JC-1 working solution at 37 °C for 30 min, and then washed twice with PBS. After washing, JC-1 imaging buffer was added and fluorescence images were collected by using a confocal laser-scanning microscope (Nikon, Tokyo, Japan) at 488 nm (excitation)/500–550 nm (emission) and 561 nm (excitation)/560–610 nm (emission). At least 300 cells from three independent experiments were counted for each group, and the fluorescence intensity of each cell was measured using ImageJ software. The ratio of red/green fluorescence was used as an indicator of mitochondrial membrane potential.

2.11. Immunoprecipitation analysis

For immunoprecipitation analysis, protein A-sepharose was prepared by suspending protein A-sepharose CL-4B (50%, v/v) in phosphate-buffered saline (PBS) at 4 °C. Brain tissue or cell extracts containing 500 μg of protein were incubated with 5–10 μg antibody (FABP3, FABP5, BAX, or VDAC-1) for 4 h at 4 °C. The mixture was further incubated with protein A-sepharose overnight at 4 °C with gentle shaking. The samples were then washed three times with PBS and separated by SDS-PAGE using commercially available gels (Cosmo Bio Co., Ltd).

2.12. Western blot analysis

Mouse coronal sections or cells were harvested and homogenized in lysis buffer (50 mM Tris–HCl pH 7.4, 0.5% Triton X-100, 4 mM EGTA, 10 mM EDTA, 1 mM Na_3VO_4, 40 mM $Na_2P_2O_7{\cdot}10\ H_2O$, 50 mM NaF, 100 nM calyculin A, 50 μg/mL leupeptin, 25 μg/mL pepstatin A, 50 μg/mL trypsin inhibitor, and 1 mM dithiothreitol). The samples were then centrifuged at 15,000 rpm for 10 min at 4 °C to collect the supernatants. Protein concentrations were determined using Bradford assays. Then, the samples were boiled for 3 min at 100 °C in 6 × Laemmli's sample buffer [31].

For electrophoresis, equal amounts of protein were loaded onto 15% SDS-PAGE gels. After separation, the bands were transferred to a polyvinylidene difluoride membrane. After blocking with T-TBS solution (50 mM Tris–HCl, pH 7.5, 150 mM NaCl, and 0.1% Tween 20) containing 5% fat-free milk powder for 1 h at room temperature, the membranes were incubated with primary antibodies (Supplemental Table 1) overnight at 4 °C with gentle shaking. After washing, the

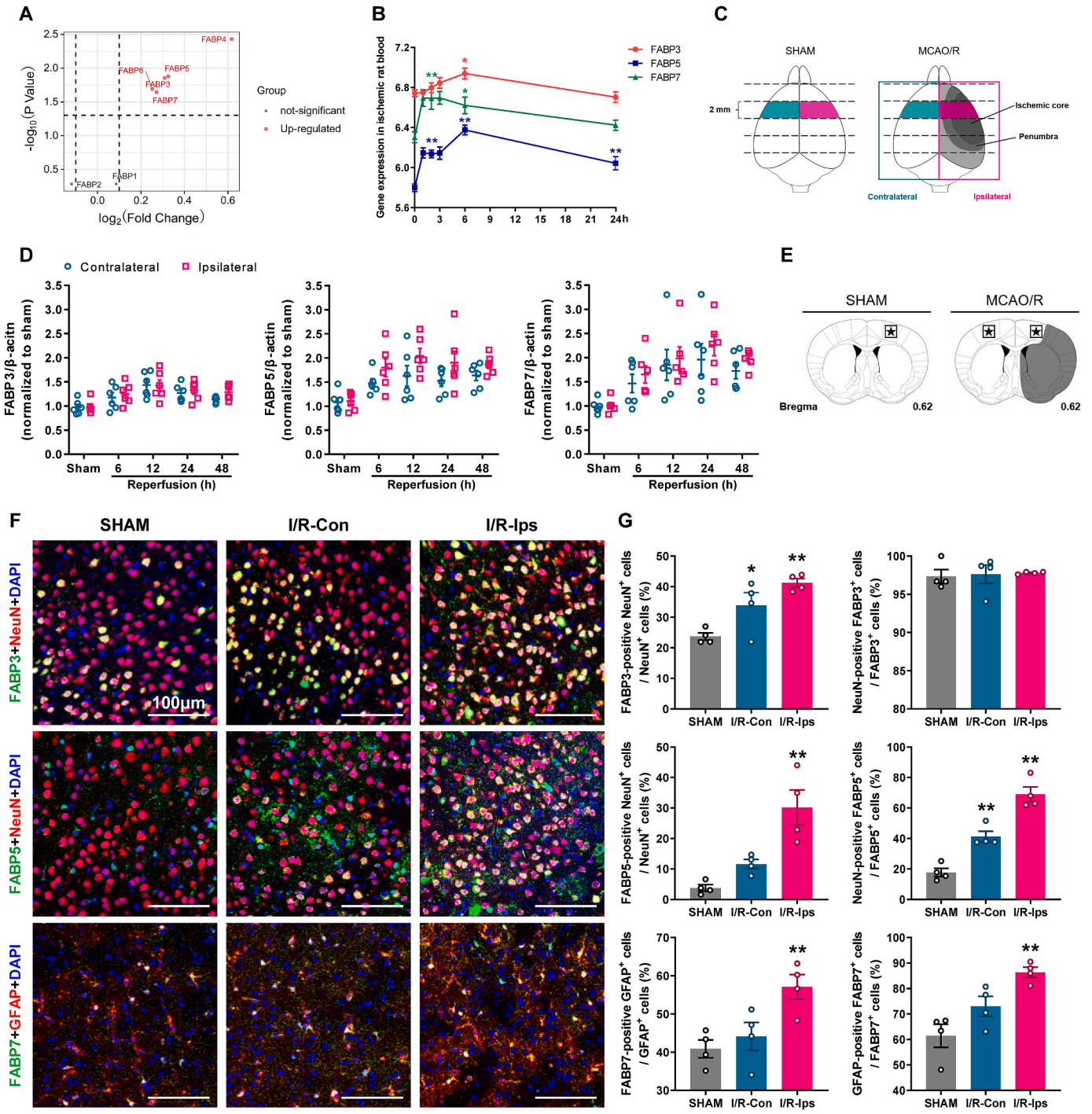

Fig. 1. Changes in FABP3, FABP5, and FABP7 expression following ischemic stroke. (A) Differentially expressed FABP genes in the blood of acute ischemic stroke patients (n = 23) were graphed in a volcano plot, with the $\log_2$ fold change on the X-axis and the $-\log_{10}$ P-value on the Y-axis. Red dots represent significantly upregulated mRNA and grey points represent non-significant mRNA. (B) Changes of FABP3, FABP5, and FABP7 mRNA in whole blood within 24 h after reperfusion in tMCAO/R rats (n = 8). (C) Schematic representation of tissues used for FABP quantification. The non-ischemic contralateral (green) and ischemic ipsilateral (pink) hemispheres were analyzed. (D) Mice were subjected to tMCAO/R. Brain tissues were collected 6, 12, 24, and 48 h after reperfusion for Western blot analysis of FABP levels. (E) Schematic diagram of the area where the immunofluorescence staining results were collected, which is marked with an asterisk (*). (F) Representative immunofluorescence staining of FABP3, FABP5, or FABP7 (green), NeuN (a neuronal marker, red), GFAP (an astrocyte marker, red), and DAPI (nuclei, blue) in sham and I/R mice. Scale bar = 100 μm. (G) The proportion of FABP3- or FABP5-expressing NeuN-positive neurons and FABP7-expressing GFAP-positive astrocytes. The proportion of FABP3-, FABP5- and FABP7-positive cells that were neurons or astrocytes is also shown. (For interpretation of the references to colour in this figure legend, the reader is referred to the Web version of this article.)

membranes were incubated with the appropriate secondary antibodies diluted in T-TBS for 2 h at room temperature. The membranes were developed using an enhanced chemiluminescence immunoblotting detection system (Amersham Biosciences, NJ, USA) and visualized using a luminescent image analyzer (LAS-4000 mini, Fuji Film, Tokyo, Japan). The band densities were analyzed using ImageJ software.

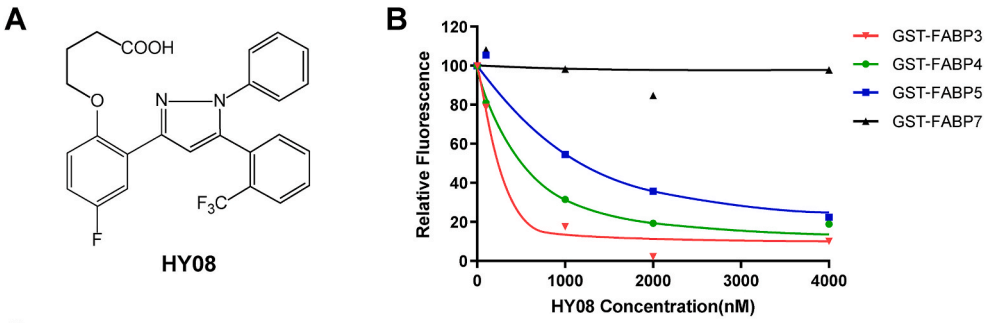

C

Kd values (nM) of HY08 derivatives on FABPs

	GST-FABP3	GST-FABP4	GST-FABP5	GST-FABP7
AA	212 ± 25[a]	301 ± 121[a]	228 ± 43[a]	28 ± 14[b]
DHA	3,387 ± 261[a]	2,326 ± 205[a]	1,783 ± 268[a]	–
BMS309403	>100,000[a]	552 ± 58[a]	3,023 ± 643[a]	–
HY08	24 ± 7	238 ± 46	410 ± 70	>100,000

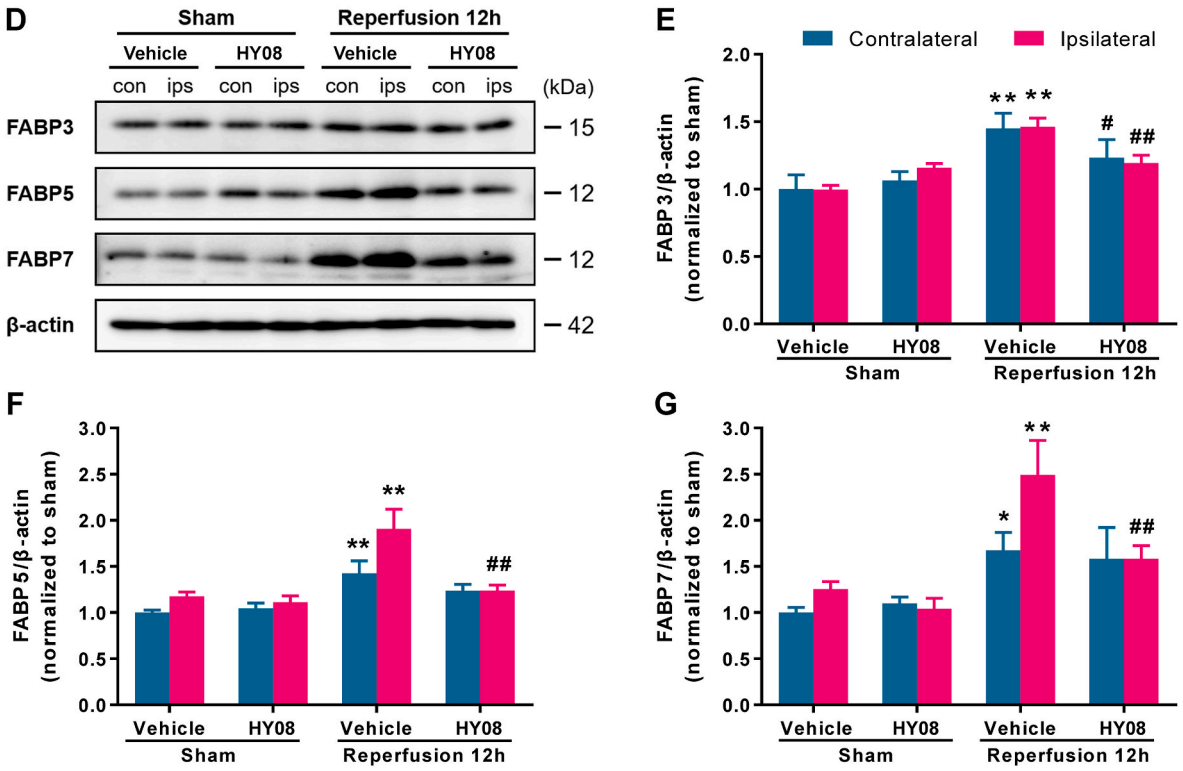

Fig. 2. Effect of HY08 on FABP expression in I/R mice. (A) Chemical structure of HY08. (B) ANS displacement assay of HY08 derivatives and GST-FABPs. The fluorescent probe ANS (4 μM) was mixed with GST-FABP in the presence 0, 100, 1000, 2000, or4000 nM HY08. The fluorescence intensity was measured at 460 nm. (C) The K_d values of HY08 to FABPs were measured via ANS assay. (D) Representative Western blots. I/R mice were treated with 0.3 mg/kg MF6 at 30 min after reperfusion. 12 h after reperfusion, brain tissues were used for Western blot analysis of FABP levels. Quantitative analyses of FABP3 (E), FABP5 (F), and FABP7 (G) protein expression levels in contralateral and ipsilateral brain tissues. The data shown in each column represent the mean ± SEM. $^{*}p < 0.05$, $^{**}p < 0.01$ vs. the vehicle-treated sham group (contralateral/ipsilateral); $^{\#}p < 0.05$, $^{\#\#}p < 0.01$ vs. the vehicle-treated I/R group (contralateral/ipsilateral) (n = 6 per group).

2.13. Immunofluorescence staining

Immunofluorescence staining was performed as previously described [26]. Mice were anesthetized and transcardially perfused with ice-cold PBS, followed immediately with 4% PFA. The brains were removed and fixed in 4% PFA overnight at 4 °C. Then, the tissues were cut into 50-μm coronal sections using a vibratome (Dosaka EM Co. Ltd., Kyoto, Japan). The sections were washed in PBS for 30 min, permeabilized in PBS containing 0.1% Triton X-100 for 2 h and blocked in PBS containing 1% BSA and 0.3% Triton X-100 for 1 h at room temperature. The sections were then incubated with primary antibodies in blocking solution for 3 days at 4 °C. After washing with PBS, brain sections were incubated with Alexa Fluor-conjugated secondary antibodies overnight at 4 °C. After extensive washing with PBS, the brain sections were mounted on slides using Vectashield (Vector Laboratories, Inc., Burlingame, CA, USA). Immunofluorescence images were obtained using a confocal

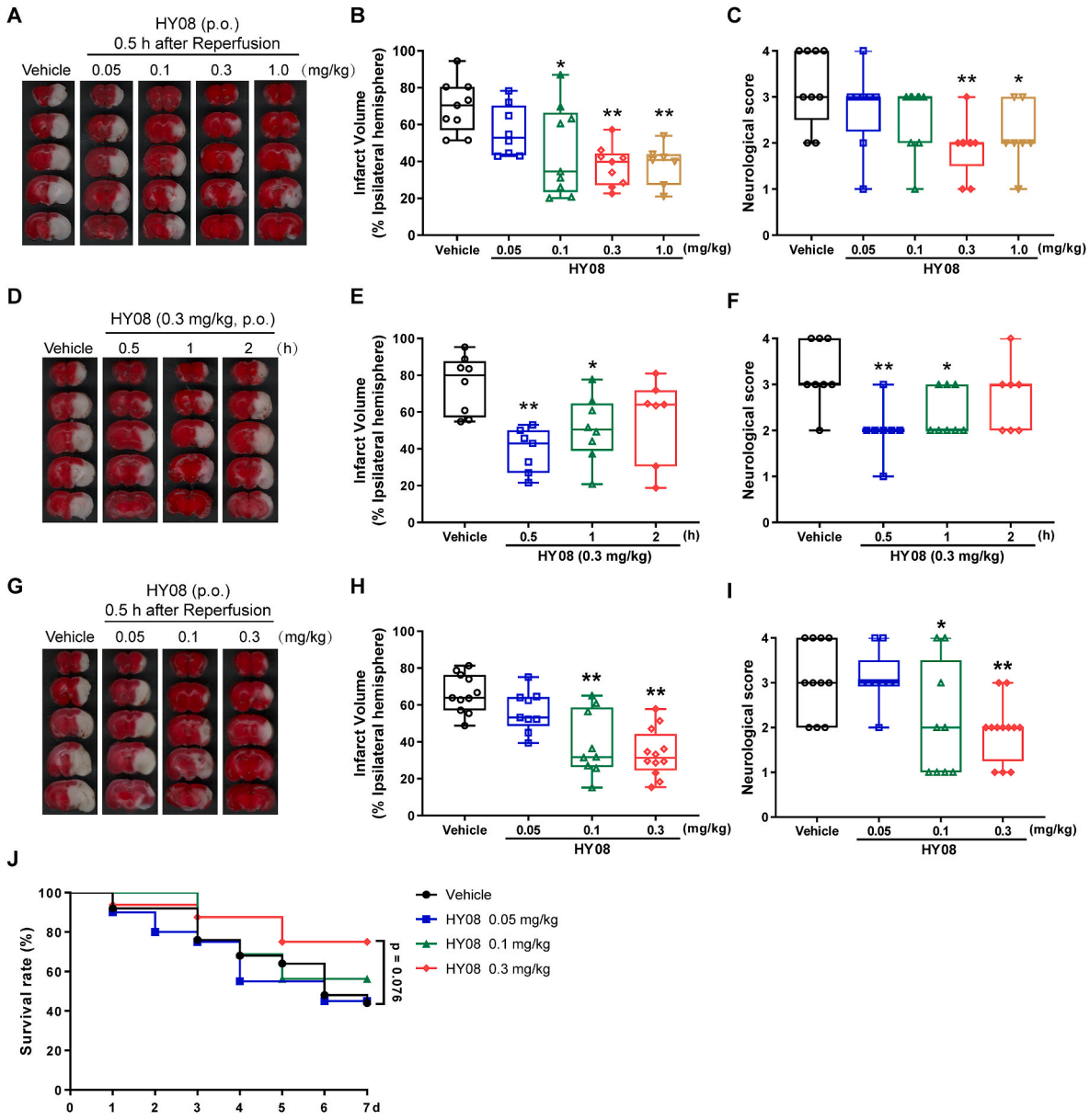

Fig. 3. Effect of HY08 on I/R injury in mice. Mice were subjected to tMCAO for 2 h. (A–C) HY08 was administrated at different concentrations (0.5, 0.1, 0.3 or 1.0 mg/kg) 30 min after reperfusion. Representative images of TTC staining (A), quantitative analysis of the infarct volumes (B), and neurological deficits (C) at 24 h after reperfusion (n = 7–9). (D–F) HY08 (0.3 mg/kg) was administrated 0.5, 1, or 2 h after reperfusion. Representative TTC staining (D), quantitative analysis of infarct volumes (E), and neurological deficits (F) at 24 h after reperfusion (n = 7–8). (G–J) HY08 was administrated with different concentrations (0.5, 0.1, 0.3 mg/kg) 30 min after reperfusion. Representative TTC staining (G), quantitative analysis of infarct volume (H), and neurological deficits (I) at day 7 after reperfusion. The number of live mice per day in each group was recorded and the survival rate (J) was calculated (n = 9–12). The data shown in each column represent the mean ± SEM. *$p < 0.05$, **$p < 0.01$ vs. the vehicle-treated I/R group.

laser-scanning microscope (Nikon, Tokyo, Japan).

SH-SY5Y cells were cultured on glass coverslips in 12-well plates (Corning, Glendale, AZ, USA) and fixed in 4% PFA for 10 min at room temperature. For mitochondrial staining, cells were treated with 0.1 mM MitoTracker Red CMXRos dye (M7512; Invitrogen) in DMEM without FBS for 30 min at 37 °C before fixation. The cells were rinsed in PBS, permeabilized with 0.1% Triton X-100 in PBS for 10 min, and blocked in 1% BSA in PBS for 30 min at room temperature. Cells were incubated with primary antibodies at 4 °C overnight. After three washes with 1% BSA/PBS, cells were incubated with secondary antibodies for 2 h at 4 °C.

2.14. Statistical analysis

All data were analyzed using SigmaPlot version 14 (SYSTAT Software Inc., San Jose, CA, USA) and are expressed as mean ± standard error of the mean (SEM). Data from all experiments were analyzed by one-way analysis of variance (ANOVA) followed by Dunnett's test for multiple comparisons or two-way ANOVA followed by Student–Newman–Keuls test for multiple comparisons. $p < 0.05$ was considered significantly different.

3. Results

3.1. FABP3, FABP5, and FABP7 expression levels were increased in I/R mouse brains

We first examined changes in FABP levels following ischemic stroke. Whole-genome Affymetrix microarray analysis revealed that FABP3,

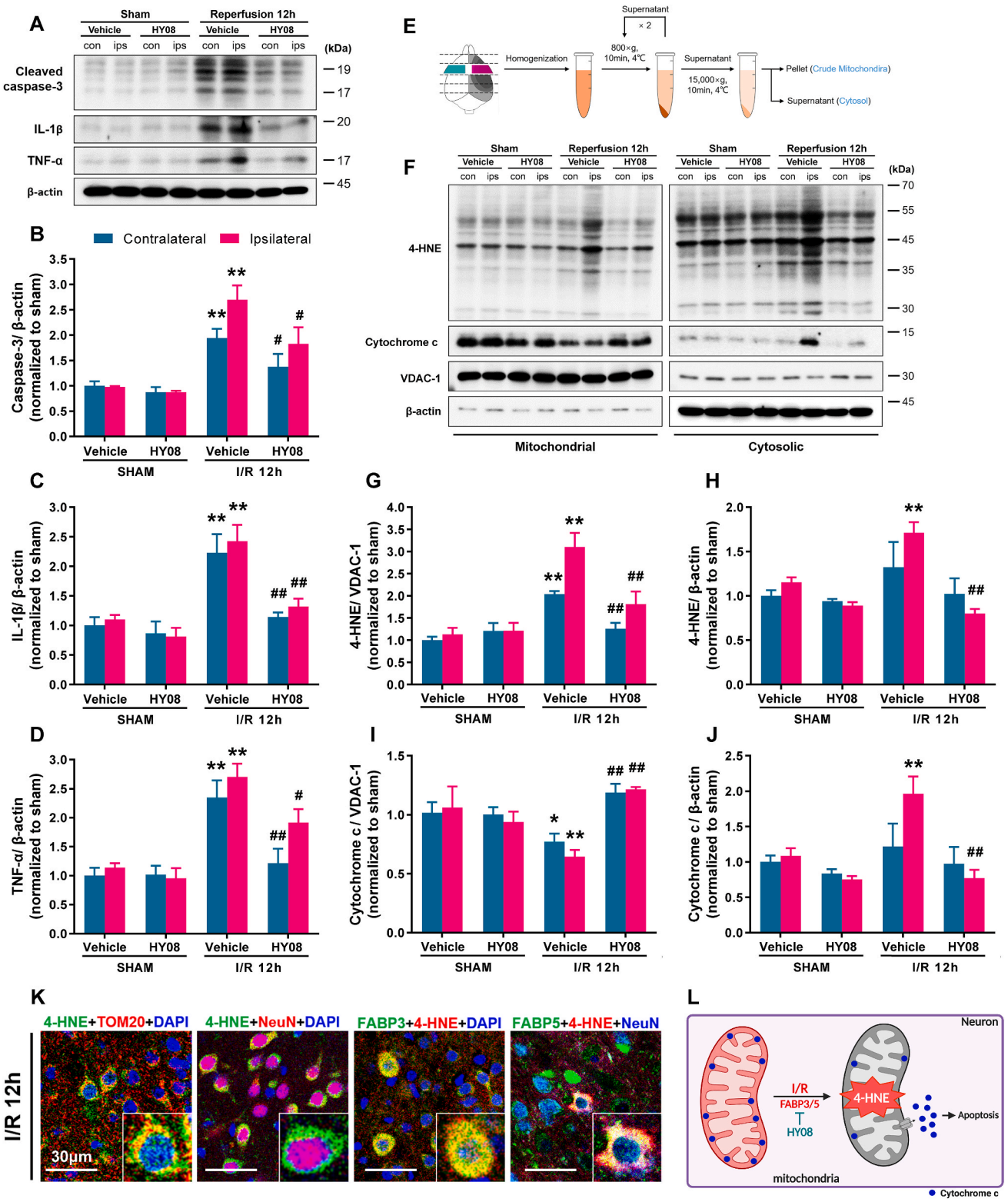

Fig. 4. HY08 reduces pro-inflammatory cytokine expression, oxidative stress, and apoptosis in I/R mice. (A–D) Representative Western blots (A). Quantitative analyses of cleaved caspase-3 (B), IL-1β (C), and TNF-α (D) protein expression in contralateral and ipsilateral brain regions (n = 4). (E) Schematic diagram of mitochondrial isolation from brain tissue. (F–J) Representative Western blots (F). Quantitative analyses of 4-HNE (G and H) and cytochrome *c* (I and J) protein expression in the mitochondrial fraction (with VDAC-1 as the internal reference) and the cytosolic fraction (with β-actin as the internal reference) in contralateral and ipsilateral brain tissues (n = 4). The data shown in each column represent the mean ± SEM. $^{*}p < 0.05$, $^{**}p < 0.01$ vs. the vehicle-treated sham group (contralateral/ipsilateral); $^{\#}p < 0.05$, $^{\#\#}p < 0.01$ vs. the vehicle-treated I/R group (contralateral/ipsilateral). (K) Representative immunofluorescence staining of 4-HNE (green), TOM20 (a mitochondrial marker) or NeuN (red), and DAPI (blue); FABP (green), 4-HNE (red), and DAPI or NeuN (blue) in I/R mice. Scale bar = 30 μm. (L) Schematic diagram of HY08 inhibition of mitochondria-related apoptosis pathways during ischemic injury. (For interpretation of the references to colour in this figure legend, the reader is referred to the Web version of this article.)

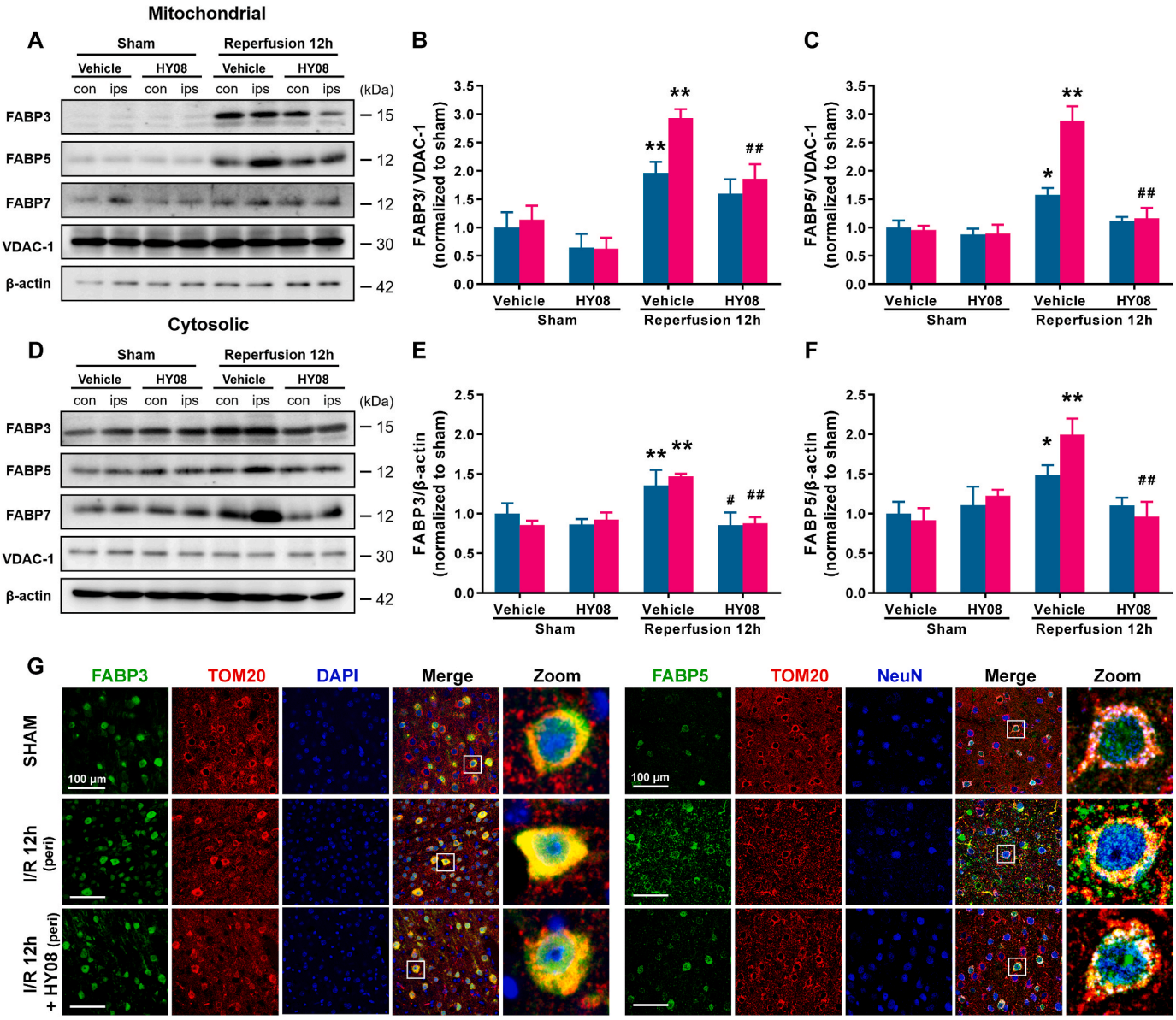

Fig. 5. FABP3 and FABP5, but not FABP7, accumulate in the mitochondria of ischemic neurons. (A–C) Representative Western blots (A). Quantitative analyses of FABP3 (B) and FABP5 (C) protein expression in the mitochondrial fraction. (D–F) Representative Western blots (D). Quantitative analyses of FABP3 (E) and FABP5 (F) protein expression in the cytosolic fraction. The data shown in each column represent the mean ± SEM. $^{*}p < 0.05$, $^{**}p < 0.01$ vs. vehicle-treated sham group (contralateral/ipsilateral); $^{\#}p < 0.05$, $^{\#\#}p < 0.01$ vs. vehicle-treated I/R group (contralateral/ipsilateral) (n = 4). (G) Representative immunofluorescence staining of FABP3 (green), TOM20 (red) and DAPI (blue); FABP5 (green), TOM20 (red) and NeuN (blue) in cortical penumbra of I/R mice. Scale bar = 100 μm. (For interpretation of the references to colour in this figure legend, the reader is referred to the Web version of this article.)

FABP5, and FABP7 mRNA levels were elevated in blood samples from patients with cardioembolic stroke compared to controls without symptomatic vascular diseases (original data are from Gene Expression Omnibus [GSE58294]) (Fig. 1A). A similar trend was observed in blood samples from rats with middle cerebral artery occlusion [GSE119121] (Fig. 1B). Next, we examined whether changes in FABP expression were the same in the brain tissue of mice with cerebral ischemia-reperfusion. FABP3, FABP5, and FABP7 protein expression in the ischemic hemisphere (ipsilateral) significantly increased with prolonged reperfusion time, especially FABP5 and FABP7. The expression of these proteins were also elevated in the non-ischemic hemisphere (contralateral) (Fig. 1D).

When we analyzed the cell types that express FABPs, we discovered that FABP3 and FABP5 were expressed and elevated in neurons in the ischemic penumbra of the cortex, whereas FABP7 was not (Fig. 1F). Almost all FABP3 was expressed in neurons, with 43.4% of neurons in the ischemic penumbra region expressing FABP3. FABP5 changes were more pronounced, with the proportion of FABP5-expressing neurons increasing from 3.78% before ischemia to 30.2% after ischemia. 69.0% of FABP5-positive cells were neurons compared to 17.7% before ischemia. FABP7 was mostly present in astrocytes in the ischemic area. Approximately 86.4% of FABP7-positive cells were GFAP-positive astrocytes. Furthermore, 57.1% of GFAP-positive astrocytes expressed FABP7, compared to 61.5% and 40.1% before ischemia, respectively (Fig. 1G). Together, these findings indicate that FABP3 and FABP5 are active in ischemic neurons, whereas FABP7 is overexpressed in astrocytes following I/R.

3.2. *FABP3 and FABP5 inhibitor, HY08 suppressed the upregulation of FABPs protein in I/R mice*

FABP3 and FABP5 are abnormally active in neurons, indicating that

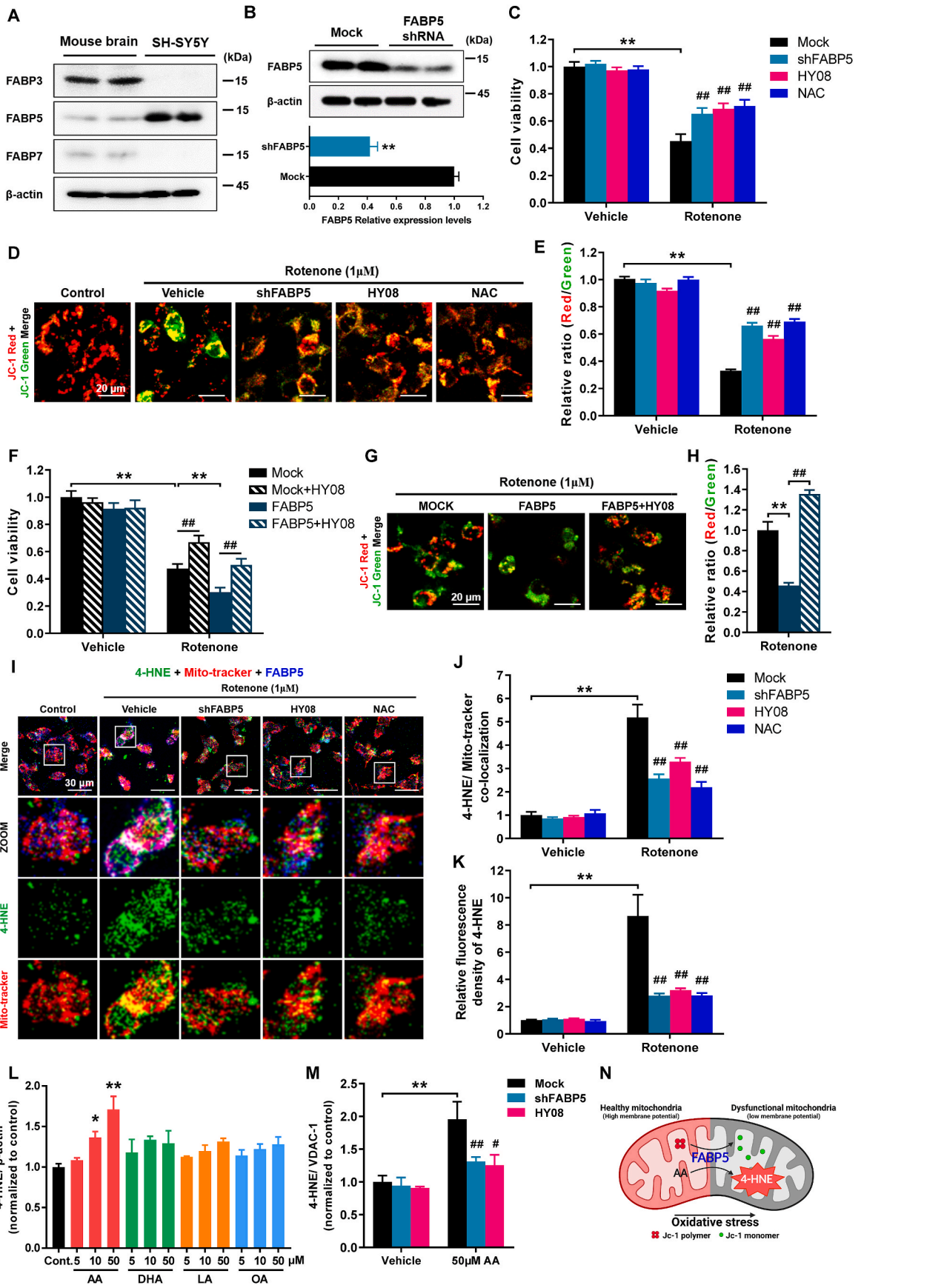

(caption on next page)

Fig. 6. FABP5 is involved in mitochondrial damage and lipid peroxidation in SH-SY5Y cells. (A) Representative Western blots of FABPs and β-actin in mouse brains and SH-SY5Y cells. (B) Quantitative analyses of FABP5 protein expression in cells transfected with FABP5 shRNA (n = 4). (C) SH-SY5Y cell viability was assessed using CCK-8 assays. Tested cells were pcDNA 3.1-transfected cells (mock, HY08, and NAC) and FABP5 shRNA-transfected cells (shFABP5) (n = 8) (D and E) Representative images of JC-1 green and red fluorescence in SH-SY5Y cells (D). Scale bar = 20 μm. Quantification of the ratio of the red to green JC-1 fluorescence intensity (E, n = 300 cells). Data are presented as mean ± SEM of 300 cells counted per group. (F) SH-SY5Y cell viability after transfection with pcDNA 3.1 (mock) or FABP5 overexpression plasmid (FABP5) (n = 8) (G and H) Representative images of green and red JC-1 fluorescence (G) and quantification of the ratio of JC-1 fluorescence intensities in FABP5-overexpressing SH-SY5Y cells (H, n = 300 cells). Data are presented as mean ± SEM of 300 cells counted per group. (I–K) Representative immunofluorescence staining of 4-HNE (green), Mito-tracker (red), and FABP5 (blue) in rotenone-treated SH-SY5Y cells (I). Scale bar = 30 μm. 4-HNE and Mito-tracker co-localization (J) and 4-HNE fluorescence intensity (K) were quantified using Image J software (n = 4). $^{*}p < 0.05$, $^{**}p < 0.01$ vs. vehicle-treated mock group; $^{\#\#}p < 0.01$ vs. rotenone-treated mock group. (L) Quantification of intracellular 4-HNE levels in fatty acid (AA, DHA, LA or AO)-treated SH-SY5Y cells (n = 3). $^{*}p < 0.05$, $^{**}p < 0.01$ vs. control cells. AA: arachidonic acid, DHA: docosahexaenoic acid, LA: linoleic acid, OA: oleic acid. (M) Quantification of mitochondrial 4-HNE levels in AA (50 μM)-treated SH-SY5Y cells in the presence or absence of HY08 (or FABP5 shRNA) (n = 3). $^{**}p < 0.01$ vs. vehicle-treated mock group; $^{\#}p < 0.05$, $^{\#\#}p < 0.01$ vs. AA-treated mock group. The data shown in each column represent the mean ± SEM. (N) Schematic diagram of the involvement of FABP5 in reducing membrane potential and lipid peroxidation during oxidative stress. (For interpretation of the references to colour in this figure legend, the reader is referred to the Web version of this article.)

they may be directly related to ischemic neuronal death. Therefore, we synthesized and screened a novel FABP3/FABP5 inhibitor, HY08, and analyzed its effects. The binding affinity of HY08 for FABPs was measured using ANS assays (Fig. 2B). HY08 exhibited strong affinity for FABP3 ($K_d = 24 \pm 7$ nM), FABP4 ($K_d = 238 \pm 46$ nM) and FABP5 ($K_d = 410 \pm 70$ nM), similar to the FABP endogenous ligand AA but had no affinity for FABP7 (Fig. 2C). Next, we tested whether HY08 could block FABP3, FABP5, and FABP7 activation 12 h after reperfusion. HY08 slightly attenuated the increased FABP3 and FABP5 protein expression in the ipsilateral ischemic area (ipsilateral) (Fig. 2D–F). Interestingly, FABP7 expression was significantly suppressed by HY08 (Fig. 2G), suggesting that FABP3 and/or FABP5 may play a role in regulating FABP7 gene expression. These findings indicate that the FABP inhibitor HY08 has a potent inhibitory effect on I/R-induced FABP expression.

3.3. HY08 reduced infarct volumes and ameliorated neurological deficits in I/R mice

We next examined the effect of HY08 on cerebral ischemic injury in mice. Mice were treated with HY08 (0.05, 0.1, 0.3 or 1.0 mg/kg) 30 min after reperfusion. I/R mice had substantial infarct volumes (69.7 ± 4.7%), which were significantly dose-dependently reduced by HY08 (0.3 mg/kg group: 37.6 ± 3.7%; 1.0 mg/kg group: 38.5 ± 4.1%; Fig. 3A and B). Moreover, neurological deficits in HY08-treated I/R mice were significantly decreased compared with those in the I/R group without HY08 (Fig. 3C). Next, we tested the optimal timing for HY08 treatment after reperfusion. HY08 treatment 30 min after reperfusion was more efficacious than HY08 treatment 1 or 2 h after reperfusion (Fig. 3D–F).

Then, we evaluated the degree of brain injury one week after reperfusion to examine the duration of the ameliorative effects of HY08 on I/R mice. Despite some mortality, only one dose showed good efficacy, persistence, and reduced ischemic brain injury. 0.3 mg/kg HY08 relieved cerebral infarction and neurological deficits 7 days after reperfusion (Fig. 3H and I) while also preventing ischemic event-related death in mice (Fig. 3J). These results suggest that HY08 protects against I/R-induced brain injury. Considering that the effects of 0.3 mg/kg HY08 were stronger and long-lasting, we chose 0.3 mg/kg as the optimum concentration for subsequent experiments.

3.4. HY08 treatment reduced IR-induced inflammation, lipid peroxidation, and apoptosis

Thus far, our findings indicate that FABP-associated signaling is an important factor in ischemic injury. Considering that neuroinflammation and oxidative stress trigger neuronal apoptosis and death during ischemic stroke [32], we next used HY08 to investigate whether FABP3 or FABP5 is involved in these two injury mechanisms. We analyzed the protein levels of interleukin (IL)-1β and TNF-α, which are inflammation markers, and cleaved caspase-3, a cell apoptosis marker, to determine whether HY08 reduces inflammation and apoptosis in I/R mice. In both ischemic and non-ischemic tissues, active caspase-3, IL-1β, and TNF-α levels were considerably lower in HY08-treated I/R mice than in I/R mice without HY08 treatment (Fig. 4A–D). To further analyze the influence of HY08 on mitochondria-related signaling, we isolated mitochondrial and cytoplasmic fractions and examined the levels of 4-HNE, a lipid peroxidation marker, and cytochrome *c*, *a* pro-apoptotic factor (Fig. 4E and F). I/R triggered lipid peroxidation and produced large amounts of the toxic product 4-HNE, particularly in the mitochondrial fraction. In contrast, lipid peroxidation was significantly suppressed in the brains of HY08-treated mice (Fig. 4G and H). HY08 treatment also prevented cytochrome *c* release from the mitochondrial intermembrane space to the cytoplasm, thereby reducing the activation of caspase-3(Fig. 4I and J), which is consistent with the results for cleaved caspase-3 (Fig. 4B). Moreover, we observed that 4-HNE co-localized with the mitochondrial outer membrane protein TOM20 or the neuronal biomarker NeuN in neurons of I/R mice. FABP3 and FABP5 were co-localized with 4-HNE in ischemic neurons (Fig. 4K). These observations reveal that FABP3 and FABP5 are involved in mitochondria-related lipid peroxidation and apoptosis pathways in ischemic neurons (Fig. 4L).

3.5. FABP3 and FABP5, but not FABP7, accumulated in the mitochondria of I/R mice

The fluorescence co-localization results in Fig. 4L show that FABP3 and FABP5 co-localize with 4-HNE in the mitochondria, indicating that FABP3 and FABP5 are located in the same mitochondrial compartment. We subsequently assessed FABP levels in the mitochondria using the same method (Fig. 4E). We found that FABP3, FABP5, and FABP7 co-localize in the cytoplasm, but are not localized to the mitochondria. Upon ischemic stimulation, some FABP3 and FABP5 accumulated in the mitochondria, whereas FABP7 did not (Fig. 5A–C). Cytoplasmic FABP3, 5, and 7 protein also increased (Fig. 5D–F), confirming the results shown in Fig. 1D. Increased FABP3, 5, and 7 expression in the mitochondria and cytoplasm was suppressed by HY08. Furthermore, immunofluorescence staining for FABP3 and 5 in ischemic neurons revealed mitochondrial localization (Fig. 5G). Nearly all FABP3 was expressed in neurons and co-localized with TOM20 in the cortical penumbra of I/R mice, while FABP5 co-localized with TOM20 in neurons ($NeuN^{+}$ cells). However, this phenomenon was decreased in sham mice and HY08-treated I/R mice. Together, these results indicate that mitochondria are essential aggregation sites for FABP3 and FABP5 following ischemic stroke.

3.6. FABP5 was involved in mitochondrial damage and lipid peroxidation in SH-HY5Y cells during oxidative stress

To further clarify the correlation between FABP and mitochondria, we used SH-SY5Y cells to examine whether FABP3 and FABP5 impair mitochondrial function. We found that SH-SY5Y cells generally

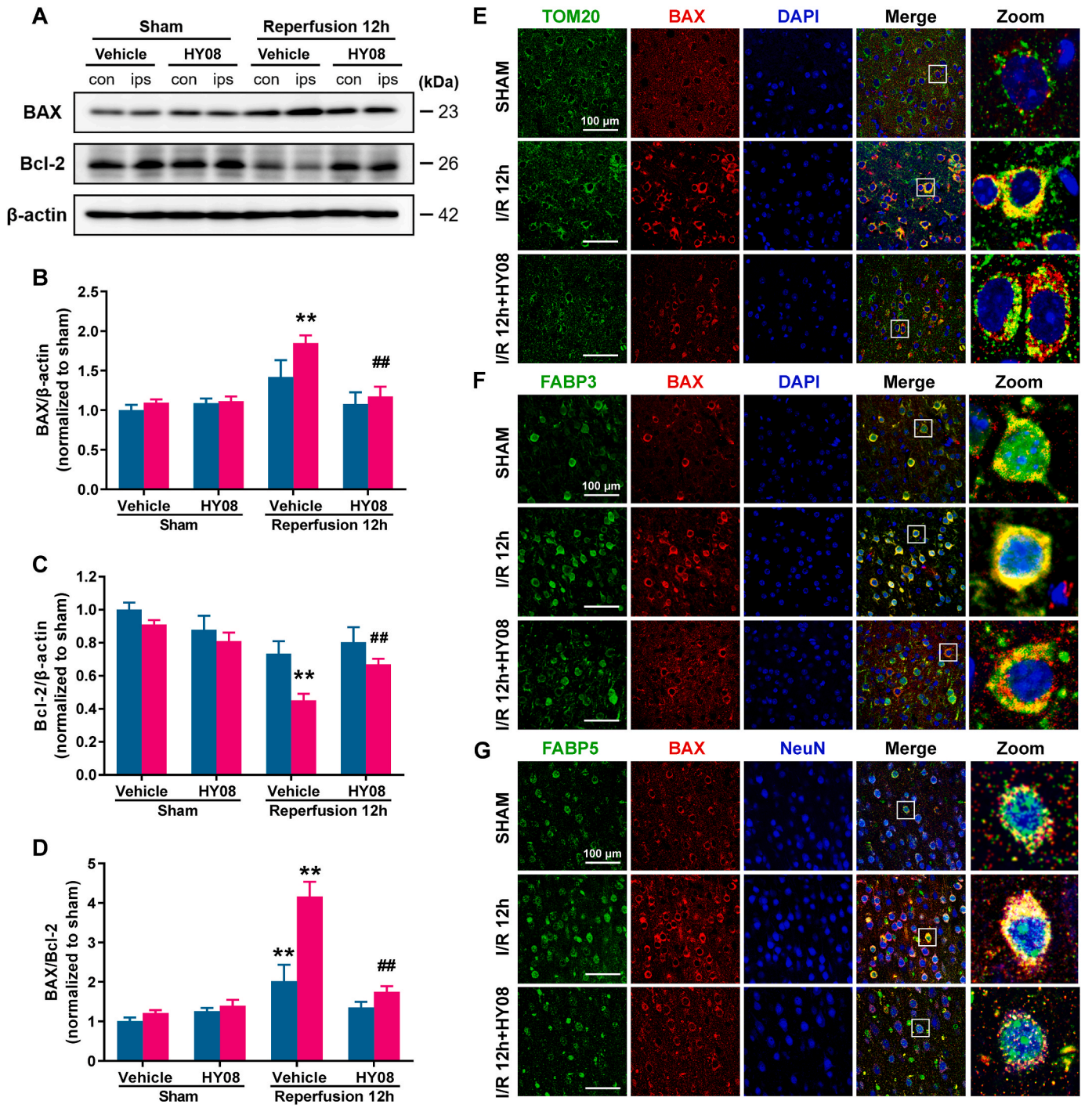

Fig. 7. HY08 treatment inhibits BAX protein expression and upregulates Bcl-2 expression in I/R mice. (A–D) Representative Western blots (A). Quantitative analyses of BAX (B) and Bcl-2 (C) protein expression and the BAX/Bcl-2 ratio (D) in contralateral and ipsilateral brain regions. The data shown in each column represent the mean ± SEM. $^{*}p < 0.05$, $^{**}p < 0.01$ vs. vehicle-treated sham group (contralateral/ipsilateral); $^{\#}p < 0.05$, $^{\#\#}p < 0.01$ vs. vehicle-treated I/R group (contralateral/ipsilateral) (n = 4). (E–G) Representative immunofluorescence staining of TOM20, FABP3, or FABP5 (green) with BAX (red) in the cortical penumbra of HY08-treated or untreated I/R mice. Scale bar = 100 μm. (For interpretation of the references to colour in this figure legend, the reader is referred to the Web version of this article.)

expressed endogenous FABP5 protein, with a small amount of FABP3. FABP7 was not expressed in SH-SY5Y cells (Fig. 6A). We next examined the effect of FABP5 on SH-SY5Y cell viability in the presence or absence of oxidative stress. shRNA-mediated FABP5 knockdown (KD) or FABP5 overexpression did not affect cell survival under normal conditions. During rotenone-induced oxidative stress, FABP5-KD cells showed increased cell viability (Fig. 6B and C), while FABP5 overexpression further exacerbated cell death (Fig. 6F). Next, we used JC-1 staining to determine the mitochondrial membrane potential. Mitochondria in rotenone-treated FABP5-KD cells displayed more JC-1 aggregates (red) and fewer JC-1 monomers (green), implying a higher membrane potential compared with rotenone-treated control cells (Fig. 6D and E). This result also shows that excessive FABP5 exacerbates mitochondrial membrane potential loss (Fig. 6G and H). Inhibiting FABP5 function (HY08) or treatment with a free radical scavenger, NAC, exerted inhibitory effects. In addition, FABP3 was also involved in

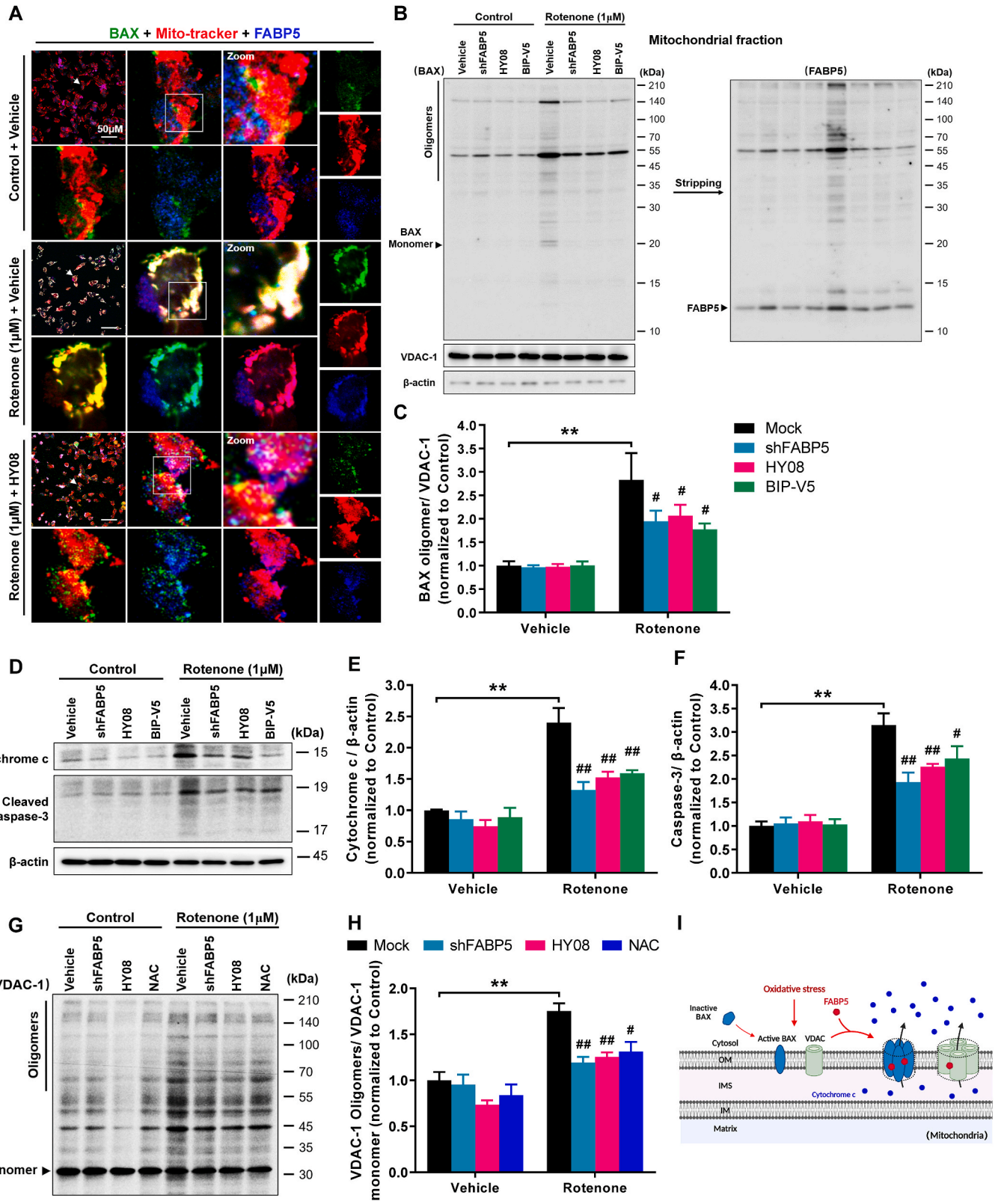

Fig. 8. FABP5 is involved in BAX and VDAC-1 oligomerization in SH-SY5Y cells. (A) Representative immunofluorescence staining of BAX (green), Mito-tracker (red), and FABP5 (blue) in rotenone-treated SH-SY5Y cells. Scale bar = 50 μm. (B and C) Representative Western blots showing BAX protein levels in mitochondrial fractions (B). Quantitative analysis of BAX oligomers (C) in SH-SY5Y cells following rotenone stimulation. (D–F) Representative Western blots (D) and quantitative analyses of cytochrome *c* (E) and cleaved caspase-3 (F) in cytosolic fractions. (G and H) Representative Western blots showing VDAC-1 protein levels in mitochondrial fractions (G). Quantitative analysis of VDAC-1 oligomers (H) in SH-SY5Y cells. The data shown in each column represent the mean ± SEM. $^{**}p < 0.01$ vs. vehicle-treated mock cells; $^{\#}p < 0.05$, $^{\#\#}p < 0.01$ vs. rotenone-treated mock cells. (n = 4). (I) Schematic diagram of the involvement of FABP5 in the formation of BAX and VDAC-1 channels in the outer mitochondrial membrane during oxidative stress. (For interpretation of the references to colour in this figure legend, the reader is referred to the Web version of this article.)

mitochondrial damage, since increased FABP3 expression further exacerbated the reduced mitochondrial membrane potential and cell death caused by rotenone (Supplemental Figs. 1A–F).

Furthermore, we examined whether FABP5 is involved in lipid peroxidation. 4-HNE, FABP5, and MitoTracker (a mitochondrial probe) were co-localized in SH-SY5Y cells. Rotenone stimulation resulted in massive intracellular 4-HNE production, particularly in FABP5-containing mitochondria (Fig. 6I). In rotenone-treated FABP5-KD cells, 4-HNE accumulation in the mitochondria was greatly reduced (Fig. 6J). The overall intracellular 4-HNE levels were similarly reduced (Fig. 6K). Furthermore, considering that free fatty acid peroxidation is an important pathway for 4-HNE generation, we examined the effects of arachidonic acid (AA, 20:4ω6), docosahexaenoic acid (DHA, 22:6ω3), linoleic acid (LA, 18:2ω-6), and oleic acid (OA, 18:1ω9) on intracellular 4-HNE levels. Although SH-SY5Y cells were treated with three different concentrations of each fatty acid, only AA (50 μM) significantly enhanced intracellular 4-HNE production (Fig. 6L). AA-induced 4-HNE accumulation in the mitochondrial fractions was significantly reduced in FABP5-KD cells (Fig. 6M), suggesting that FABP5 is involved in AA peroxidation.

Together, these findings reveal that FABP3 and FABP5 participate in neuronal apoptosis during oxidative stress by mediating mitochondrial damage. Further, our results show that FABP5 is a key player in lipid peroxidation (Fig. 6N).

3.7. FABP3 and FABP5 activated the BAX-related apoptosis pathway in I/R mice

Previous studies revealed that apoptosis-related proteins such as BAX and Bcl-2 have a major impact on ischemic neuronal death [33,34]. Ischemic tissues showed an increase in pro-apoptotic BAX protein and a concomitant decrease in anti-apoptotic Bcl-2, resulting in a significant increase in the BAX/Bcl-2 ratio, which favors cell death. HY08 treatment reversed the apoptotic trend and maintained cell survival (Fig. 7A–D). Since BAX moved from the cytoplasm to the outer mitochondrial membrane during apoptosis (Fig. 7E), we examined whether FABP3 or FABP5, which also accumulate in the mitochondria, co-localized with BAX. In the ischemic penumbra, both FABP3 and FABP5 co-localized with BAX in neurons (Fig. 7F and G). To confirm the binding of FABP3 and FABP5 proteins to BAX protein, we investigated their interactions using co-immunoprecipitation. Consistently, BAX protein bound to FABP3 and FABP5. Isolated FABP3 or FABP5 protein was also linked to BAX (Supplemental Fig. 2A). However, in the presence of HY08, the FABP3/5 and BAX interactions were significantly disrupted (Supplemental Figs. 2B–E). These findings suggest that FABP3 and FABP5 migrate to the mitochondria, bind to BAX, and participate in BAX-related signaling. Further, our results suggest that HY08 inhibits apoptotic signaling by blocking interactions between FABP3/5 and BAX.

3.8. FABP5 mediated BAX and VDAC-1 oligomerization to form mitochondrial outer membrane pores and release cytochrome c in vitro

To further determine whether FABP5 is an essential factor that triggers BAX oligomer formation, we examined the impact of inhibiting or knocking down FABP5 on BAX conformational changes and associated signaling under oxidative stress. Following rotenone stimulation, BAX was overexpressed and moved to FABP5-containing mitochondria in SH-SY5Y cells. However, these alterations were significantly attenuated when FABP5 was blocked by HY08 (Fig. 8A). Rotenone-treated cells showed higher levels of BAX oligomers in the mitochondrial fractions. When the same membranes were blotted with FABP5 antibody after stripping, we found greater FABP5 levels in BAX oligomers (Fig. 8B), indicating that FABP5 is indeed involved in BAX oligomer formation. Following treatment with FABP5 shRNA, HY08, or the BAX inhibitor BIP-V5, BAX oligomerization was reduced (Fig. 8C), mitochondrial outer membrane pores failed to develop, and cytochrome *c* was not released (Fig. 8D and E). Caspase-3 activation was also suppressed (Fig. 8F). These results suggest that FABP5 plays a role in the BAX-related apoptotic pathway. Considering that SH-SY5Y cells do not express endogenous FABP3, we tested whether FABP3 plays a similar role to FABP5 by transfecting cells with exogenous expression plasmids. Although FABP3 expression was increased in cells without injury, it did not accumulate in the mitochondria. During rotenone-induced oxidative stress, FABP3 accumulated in the mitochondria. BAX was mostly concentrated in FABP3-located mitochondria (Supplemental Fig. 1G).

Because mitochondrial pores can also form from VDAC-1 oligomers, we also investigated the effects of FABP5 on VDAC-1 oligomer levels in rotenone-treated SH-SY5Y cells. FABP5 shRNA treatment resulted in fewer VDAC-1 oligomers than in control cells (Fig. 8G and H). We also observed a structural connection between FABP5 and VDAC-1 (Supplemental Fig. 3A), indicating that FABP5 is directly involved in the VDAC-1 pore formation. HY08 treatment blocked oxidative stress-induced interactions between VDAC-1 and FABP5, thereby inhibiting VDAC-1 oligomerization (Fig. 8H and Supplementary Figs. 3B and C).

Collectively, FABP5 is involved in mitochondrial pore formation in neuronal cell models of oxidative stress by promoting BAX and VADC-1 oligomerization (Fig. 8I). FABP3 may also be involved, at least through the BAX pathway. Inhibiting FABP3 and FABP5 with HY08 reduces mitochondrial apoptotic signaling, thereby rescuing neuronal cells.

4. Discussion

Our main objective was to determine the role of FABPs in ischemic neuronal death. FABP3 and FABP5 were significantly elevated in ischemic neurons in the penumbra region after I/R. These proteins are implicated in damage from mitochondria-related oxidative stress and apoptosis in neurons. The FABP3/5 inhibitor HY08 exerts neuroprotective effects against ischemic neuronal death, suggesting that FABP3 and FABP5 play a role in inducing apoptosis in ischemic stroke.

We observed a significant association between FABPs and ischemic neurons *in vivo*. Although FABP3, 5, and 7 expression was elevated in ischemic areas, FABP7 was not expressed in ischemic neurons. In addition, FABP3 and FABP5, particularly FABP5, were elevated in ischemic neurons, implying that FABP3 and FABP5 may be directly involved in mitochondrial injury and neuronal apoptosis. This conclusion is based on previous studies that showed that increased FABP3 expression enhances cardiomyocyte apoptosis during myocardial infarction [35] and that FABP5 expression is elevated in apoptotic CA1 neurons following ischemia [36]. Interestingly, although FABP3 is almost exclusively expressed in neurons [37], brain ischemia only slightly enhanced neuronal FABP3 expression. In contrast, the number of FABP5-positive neurons was dramatically increased ($NeuN^+$+$FABP5^+$/$FABP5^+$, 17.7%–69.0%, Fig. 1G), suggesting pivotal roles of FABP5 in mitochondrial injury. FABP7 overexpression in glial cells from amyotrophic lateral sclerosis mice triggers NF-κB-driven pro-inflammatory responses in astrocytes [25]. Additionally, FABP7 is involved in hippocampal astrocyte proliferation following ischemia [36]. Consistent with previous studies, FABP7 was highly expressed in astrocytes after ischemia, suggesting that FABP7 indirectly mediates neuronal death via astrocyte-mediated inflammatory responses.

To better understand the relationship between FABPs and ischemic injury, we previously investigated the effects of highly specific FABP7 inhibitor, which alleviates ischemic brain injury by blocking inflammation-associated microsomal prostaglandin E synthase-1 (mPGES-1)-prostaglandin E2 (PGE_2) signaling [26]. Our previous results show a critical role of FABP7 in neuroinflammation. In this study, we focused on FABP3 and FABP5 functions in ischemic neurons using HY08, a novel FABP3/5 inhibitor. HY08 has a K_d value of 24 ± 7 nM. Although HY08 showed no affinity for FABP7, it moderately inhibited FABP4 ($K_d = 238 \pm 46$ nM) and FABP5 ($K_d = 410 \pm 70$ nM). This implies that HY08 could also inhibit FABP4 and FABP5 functions. HY08 significantly inhibited FABP5-induced mitochondrial injury and neuron

loss (Fig. 6). Moreover, HY08 treatment effectively prevented neuronal mortality in I/R mice. Notably, FABP3 and FABP5 accumulate in the mitochondria of ischemic neurons. Furthermore, previous studies demonstrate that FABP3 overexpression reduces mitochondrial activity and causes abnormal mitochondrial morphology in embryonic cancer cells [38]. FABP3 is also involved in the loss of mitochondrial activity during dopamine neuron degeneration [39]. FABP5 inhibitors reduce mitochondrial injury in KG-1C glia cells treated with the cytotoxic sphingolipid psychosine [40] and oxidatively damage α-synuclein--transfected Neuro2A cells [30]. These findings suggest that FABP3 and FABP5 are intimately associated with impaired mitochondrial function. However, how FABP4 functions in microglia after ischemia remains unclear. Microglial FABP4 regulates neuroinflammation in obese mice [41] and in human immunodeficiency virus-1-associated neurocognitive disorder [42]. Further extensive studies are required to investigate the function of FABP4 in microglia after ischemia.

Previous studies have revealed that the siRNA silencing of FABP3 reduces 4-HNE generation in palmitic acid-treated podocytes, whereas FABP3 overexpression enhances 4-HNE generation [43]. We previously investigated the effect of FABP3 on lipid peroxidation using an *in vitro* Parkinson's disease model. 1-methyl-4-phenylpyridine (MPP^+) treatment increased oxidative damage via elevated 4-HNE synthesis in primary dopaminergic neurons of wild-type mice [39]. However, MPP^+ failed to elevate 4-HNE in FABP3-deficient dopaminergic neurons. HY08 relieved oxidative stress injury in I/R mice by inhibiting FABP3 function and reducing 4-HNE levels in ischemic neurons. Rotenone, a mitochondrial complex I inhibitor, has been widely used to prepare models of Parkinson's disease [44–46]. In contrast to the limitations of *in vivo* applications caused by the large variability in the percentage and extent of nigrostriatal dopaminergic damage in animals [46,47], rotenone can directly enter cells to inhibit mitochondrial respiration [48], inducing a large amount of mitochondrial reactive oxygen species (ROS) and intracellular ROS in SH-SY5Y cells [49,50]. Following exposure to rotenone, a large number of SH-SY5Y cells undergo cell death, most likely due to severe impairment of mitochondrial function, because quantitative data of JC-1 staining showed a significantly decrease in mitochondrial membrane potential (MMP), which appeared as fewer JC-1 red aggregates and increased JC-1 green monomers. FABP5 shRNA and HY08 protected against this damage, whereas overexpression of FABP3 or FABP5 exacerbated it. However, it is important to note that the results of JC-1 measurements are only for reference purposes because JC-1 may not be suitable for MMP detection. Recent studies have shown that the calculate of the ratio of red aggregated JC-1 and green JC-1 monomers is inaccurate, and that the change of this ratio cannot be entirely attributed to changes in MMP; secondly, JC-1 aggregates may change independently of MMP, and aggregates may fail to dissolve back to the green monomer when MMP is decreased [51,52]. Furthermore, JC-1 penetrates the plasma membrane very slowly, which means that it is highly artifact-prone and likely to be misled [52,53]. Therefore, additional validation using other more effective MMP detection approaches, such as an alternative strategy to Tetramethylrhodamine methyl ester (TMRM) [52], is required.

According to the immunofluorescence results, 4-HNE was abundantly produced in rotenone-treated cells and mostly localized in neuronal mitochondria where FABP3 and FABP5 were aggregated. Furthermore, we observed that knocking down FABP5 expression decreased rotenone-induced 4-HNE production in SH-SY5Y cells. The massive accumulation of FABP3 and FABP5 in the mitochondria of ischemic neurons, as well as the significant inhibitory effects of HY08 and FABP5 knockdown on 4-HNE levels in mitochondria, suggest that FABP3/5 are involved in mitochondrial lipid peroxidation. Moreover, lipid peroxidation is the main mechanism of oxidative damage [54,55], further implying that FABP3/5 play an essential role in the promotion of oxidative damage. Furthermore, 4-HNE levels showed a significant increase in the mitochondrial fractions of ischemic tissue, but it is uncertain whether mitochondrial lipid peroxidation predominates. FABP3/5 was actively implicated in this process, however this does not mean that FABP3/5-mediated lipid peroxidation predominates in mitochondrial damage. AA is the main source of 4-HNE [56]. We hypothesized that free AA in ischemic cells is a major source of fatty acids for FABP3/5-mediated lipid peroxidation, including 4-HNE. However, it is unclear whether fatty acid transport to mitochondria by FABP3/5 is critical for lipid peroxidation.

Bcl-2 family proteins control downstream caspase activation and the mitochondrial apoptosis pathway [57,58]. In I/R mice, HY08 treatment reversed the upregulation of the pro-apoptotic BAX protein and the downregulation of the anti-apoptotic Bcl-2 protein, indicating a regulatory role for FABP3 and FABP5 in BAX-induced apoptosis. We observed FABP3/5 and BAX co-localization in ischemic neurons. This result implies that FABP3/5 affects BAX protein expression and may structurally mediate BAX-induced apoptosis. BAX/FAPB3 complexes were detected in ischemic tissue by co-immunoprecipitation (Fig. 7F). These complexes were disrupted by HY08 treatment. In addition, BAX oligomer formation in mitochondrial compartments after oxidative damage was significantly reduced by knocking down FABP5 expression or inhibiting its function (Fig. 8B and C). We could not determine whether there is a preference for FABP3 or FABP5 to induce BAX-induced pore formation. Previous studies showed that BAX oligomer channels are required for apoptosis [59] and that FABP5 is involved in BAX-induced pore formation [40]. In addition to BAX-induced pore formation, there are channels in the mitochondrial outer membrane that are constituted by VDAC-1. We recently demonstrated that FABP5 forms complexes with VDAC-1 protein and causes VDAC-1 oligomer-dependent mitochondrial macropore formation in EAE mouse neurons [60]. VDAC-1 oligomerization decreased in the presence of HY08. We found that accelerating mitochondrial outer membrane pore formation and increasing membrane permeabilization appear to be important means for FABP3/5 to affect mitochondrial function. This conclusion explains why excessive FABP can aggravate the reduction of mitochondrial membrane potential. However, although these results strongly support the contribution of FABP3 and FABP5 to oligomer formation, more direct evidence is required. In our next study, we will isolate the FABP complexes in ischemic tissue and use X-ray crystallography to further confirm FABP binding to BAX or VDAC-1.

In this study, we focused on the involvement of FABPs in ischemic neuronal apoptosis. Taken together, FABP3 and FABP5 accumulate in mitochondria of ischemic neurons, contribute to lipid peroxidation and BAX-associated apoptosis, and are key initiators of mitochondrial damage. Furthermore, we show that the FABP3/5 inhibitor HY08 protects mitochondria against ischemic injury by rescuing ischemic neurons via FABP3 and FABP5 inhibition. Importantly, HY08 showed efficient, long-lasting therapeutic effects on brain injury and neurological rehabilitation in mice with cerebral I/R. Therefore, HY08 represents a novel and potentially effective treatment for ischemic stroke.

Author contributions

Q.G., investigation and original manuscript writing; C.A., H.W., and W.J., investigation; I.K., investigation and methodology; K.F., supervision, review/editing, project administration, and funding. All authors have reviewed the final manuscript and approved the manuscript for publication.

Declaration of competing interest

The authors declare the following financial interests/personal relationships which may be considered as potential competing interests: I. K. received a research grant from Shiratori Pharmaceutical Co., Ltd. H.Y. is an employee of Shiratori Pharmaceutical Co., Ltd. K.F. is the CEO of BRI Pharma and had a role of supervision and provided a grant [grant number JP20dm0107071]. The other authors (Q.G., A.C., H.W., W.J.) declare no conflicts of interest in the present study. The HY08 compound

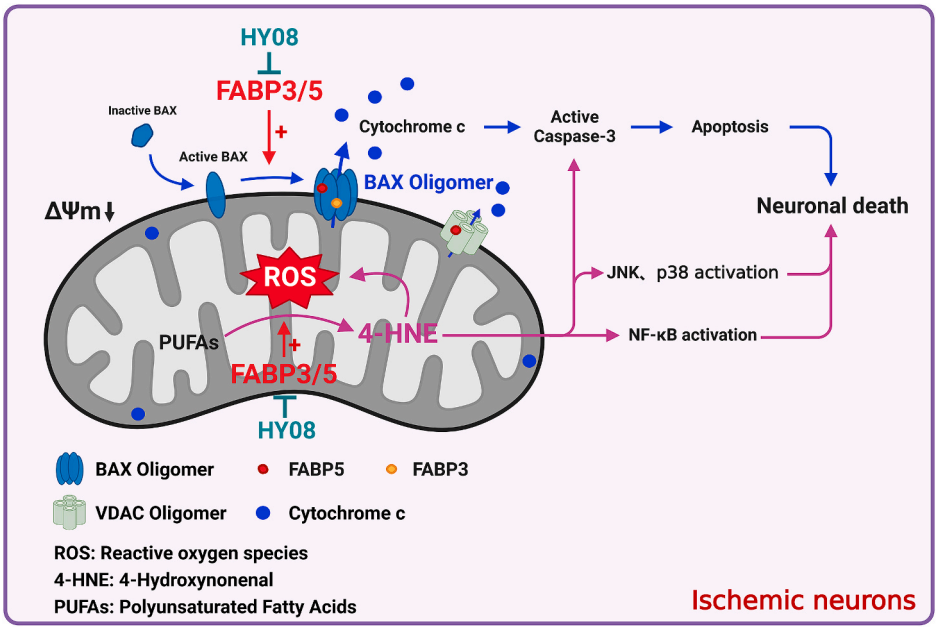

Fig. 9. Schematic diagram of the involvement of FABP3 and FABP5 in mitochondria-associated apoptosis pathways in ischemic neurons. FABP3 and FABP5 have similar mechanisms of action. These proteins exacerbate oxidative stress injury by mediating the accumulation of 4-HNE, a toxic byproduct of fatty acid peroxidation. FABP3/5 are also involved in mitochondrial BAX and VDAC channel formation, which reduces the mitochondrial membrane potential and results in apoptotic signaling. The FABP3/5 inhibitor HY08 effectively inhibits FABP function, helps mitochondria to resist ischemic damage, and enhances neuronal tolerance to ischemia. Thus, HY08 protects against mitochondrial damage and is a potential treatment for ischemic stroke.

was provided by Shiratori Pharmaceutical Co., Ltd, which owns the HY08 patent.

Data availability

Data will be made available on request.

Acknowledgements

This work was supported in part by Shiratori Pharmaceutical Co., Ltd. This work was also supported by the Japan Agency for Medical Research and Development (AMED) [grant number 22ym01 26095h0001], the Japan Society for the Promotion of Science, KAKENHI (22K06644), Takeda Science Foundation, and Smoking Research Foundation to I.K. Graphical abstract and some figures (Fig. 4E, L, Fig.6N, Figs. 8I and 9) were created with BioRender.com.

Appendix A. Supplementary data

Supplementary data to this article can be found online at https://doi.org/10.1016/j.redox.2022.102547.

Data sharing statement

The data supporting the findings of this study are available in the article and supplementary materials. The data in Fig. 1a and b were based on publicly available data from the Gene Expression Omnibus [GEO; https://www.ncbi.nlm.nih.gov/geo/query/acc.cgi?acc=GSE58294 (Fig. 1A); https://www.ncbi.nlm.nih.gov/geo/query/acc.cgi?acc=GSE119121 (Fig. 1B)]. All original data will be made available by the corresponding authors upon reasonable request.

References

[1] A.K. Boehme, C. Esenwa, M.S.V. Elkind, Stroke risk factors, genetics, and prevention, Circ. Res. 120 (3) (2017) 472–495, https://doi.org/10.1161/Circresaha.116.308398.
[2] B. Puig, S. Brenna, T. Magnus, Molecular communication of a dying neuron in stroke, Int. J. Mol. Sci. 19 (9) (2018), https://doi.org/10.3390/ijms19092834.
[3] Q.Z. Tuo, S.T. Zhang, P. Lei, Mechanisms of neuronal cell death in ischemic stroke and their therapeutic implications, Med. Res. Rev. 42 (1) (2022) 259–305, https://doi.org/10.1002/med.21817.
[4] F. Liu, J.F. Lu, A. Manaenko, et al., Mitochondria in ischemic stroke: new insight and implications, Aging Dis. 9 (5) (2018) 924–937, https://doi.org/10.14336/Ad.2017.1126.
[5] L. Gao, F. Liu, P.P. Hou, et al., Neurons release injured mitochondria as "Help-Me" signaling after ischemic stroke, Front. Aging Neurosci. 14 (2022), https://doi.org/10.3389/fnagi.2022.785761.
[6] W. Li, S. Yang, Targeting oxidative stress for the treatment of ischemic stroke: upstream and downstream therapeutic strategies, Brain Circ. 2 (4) (2016) 153–163, https://doi.org/10.4103/2394-8108.195279.
[7] X.Y. Zhou, H.M. Chen, L. Wang, et al., Mitochondrial dynamics: a potential therapeutic target for ischemic stroke, Front. Aging Neurosci. 13 (2021), https://doi.org/10.3389/fnagi.2021.721428.
[8] S.L. Zeiger, E.S. Musiek, G. Zanoni, et al., Neurotoxic lipid peroxidation species formed by ischemic stroke increase injury, Free Radic. Biol. Med. 47 (10) (2009) 1422–1431, https://doi.org/10.1016/j.freeradbiomed.2009.08.011.
[9] L.J. Su, J.H. Zhang, H. Gomez, et al., Reactive oxygen species-induced lipid peroxidation in apoptosis, autophagy, and ferroptosis, Oxid. Med. Cell. Longev. (2019), https://doi.org/10.1155/2019/5080843, 2019.
[10] W.C. Lee, H.Y. Wong, Y.Y. Chai, et al., Lipid peroxidation dysregulation in ischemic stroke: plasma 4-HNE as a potential biomarker? Biochem. Bioph. Res. Co. 425 (4) (2012) 842–847, https://doi.org/10.1016/j.bbrc.2012.08.002.
[11] X. Zhai, W. Wang, S. Sun, et al., 4-Hydroxy-2-Nonenal promotes cardiomyocyte necroptosis via stabilizing receptor-interacting serine/threonine-protein kinase 1, Front. Cell Dev. Biol. 9 (2021), 721795, https://doi.org/10.3389/fcell.2021.721795.
[12] S. Zhang, S.J. Rao, M.W. Yang, et al., Role of mitochondrial pathways in cell apoptosis during He-patic ischemia/reperfusion injury, Int. J. Mol. Sci. 23 (4) (2022), https://doi.org/10.3390/ijms23042357.
[13] T. Kuwana, L.E. King, K. Cosentino, et al., Mitochondrial residence of the apoptosis inducer BAX is more important than BAX oligomerization in promoting membrane permeabilization, J. Biol. Chem. 295 (6) (2020) 1623–1636, https://doi.org/10.1074/jbc.RA119.011635.
[14] N.B. Bloch, T.E. Wales, M.S. Prew, et al., The conformational stability of pro-apoptotic BAX is dictated by discrete residues of the protein core, Nat. Commun. 12 (1) (2021), https://doi.org/10.1038/s41467-021-25200-7.
[15] Q. Guo, I. Kawahata, A. Cheng, et al., Fatty acid-binding proteins: their roles in ischemic stroke and potential as drug targets, Int. J. Mol. Sci. 23 (17) (2022) 9648, https://doi.org/10.3390/ijms23179648.
[16] N. Shioda, Y. Yabuki, Y. Kobayashi, et al., FABP3 protein promotes alpha-synuclein oligomerization associated with 1-Methyl-1,2,3,6-tetrahydropiridine-induced neurotoxicity, J. Biol. Chem. 289 (27) (2014) 18957–18965, https://doi.org/10.1074/jbc.M113.527341.
[17] C. Shimamoto, T. Ohnishi, M. Maekawa, et al., Functional characterization of FABP3, 5 and 7 gene variants identified in schizophrenia and autism spectrum disorder and mouse behavioral studies, Hum. Mol. Genet. 23 (24) (2014) 6495–6511, https://doi.org/10.1093/hmg/ddu369.
[18] I. Kawahata, K. Fukunaga, Impact of fatty acid-binding proteins and dopamine receptors on alpha-synucleinopathy, J. Pharmacol. Sci. 148 (2) (2022) 248–254, https://doi.org/10.1016/j.jphs.2021.12.003.
[19] A. Cheng, W. Jia, I. Kawahata, et al., Impact of fatty acid-binding proteins in alpha-synuclein-induced mitochondrial injury in synucleinopathy, Biomedicines 9 (5) (2021), https://doi.org/10.3390/biomedicines9050560.

[20] D. Chiasserini, L. Biscetti, P. Eusebi, et al., Differential role of CSF fatty acid binding protein 3, alpha-synuclein, and Alzheimer's disease core biomarkers in Lewy body disorders and Alzheimer's dementia, Alzheimer's Res. Ther. 9 (1) (2017) 52, https://doi.org/10.1186/s13195-017-0276-4.
[21] C.E. Teunissen, R. Veerhuis, J. De Vente, et al., Brain-specific fatty acid-binding protein is elevated in serum of patients with dementia-related diseases, Eur. J. Neurol. 18 (6) (2011) 865–871, https://doi.org/10.1111/j.1468-1331.2010.03273.x.
[22] A. Cheng, Y.F. Wang, Y. Shinoda, et al., Fatty acid-binding protein 7 triggers alpha-synuclein oligomerization in glial cells and oligodendrocytes associated with oxidative stress, Acta Pharmacol. Sin. 43 (3) (2022) 552–562, https://doi.org/10.1038/s41401-021-00675-8.
[23] E.Y. Rao, P. Singh, Y. Li, et al., Targeting epidermal fatty acid binding protein for treatment of experimental autoimmune encephalomyelitis, BMC Immunol. 16 (2015), https://doi.org/10.1186/s12865-015-0091-2.
[24] T. Paskevicius, J. Jung, M. Pujol, et al., The Fabp5/calnexin complex is a prerequisite for sensitization of mice to experimental autoimmune encephalomyelitis, Faseb. J. 34 (12) (2020) 16662–16675, https://doi.org/10.1096/fj.202001539RR.
[25] K.M. Killoy, B.A. Harlan, M. Pehar, et al., FABP7 upregulation induces a neurotoxic phenotype in astrocytes, Glia 68 (12) (2020) 2693–2704, https://doi.org/10.1002/glia.23879.
[26] Q.Y. Guo, I. Kawahata, T. Degawa, et al., Fatty acid-binding proteins aggravate cerebral ischemia-reperfusion injury in mice, Biomedicines 9 (5) (2021), https://doi.org/10.3390/biomedicines9050529.
[27] M.L. Sun, H. Izumi, Y. Shinoda, et al., Neuroprotective effects of protein tyrosine phosphatase 1B inhibitor on cerebral ischemia/reperfusion in mice, Brain Res. 1694 (2018) 1–12, https://doi.org/10.1016/j.brainres.2018.04.029.
[28] M.L. Sun, Y. Shinoda, K. Fukunaga, KY-226 protects blood-brain barrier function through the akt/FoxO1 signaling pathway in brain ischemia, Neuroscience 399 (2019) 89–102, https://doi.org/10.1016/j.neuroscience.2018.12.024.
[29] Y. Shinoda, Y.F. Wang, T. Yamamoto, et al., Analysis of binding affinity and docking of novel fatty acid-binding protein (FABP) ligands, J. Pharmacol. Sci. 143 (4) (2020) 264–271, https://doi.org/10.1016/j.jphs.2020.05.005.
[30] Y.F. Wang, Y. Shinoda, A. Cheng, et al., Epidermal fatty acid-binding protein 5 (FABP5) involvement in alpha-synuclein-induced mitochondrial injury under oxidative stress, Biomedicines 9 (2) (2021), https://doi.org/10.3390/biomedicines9020110.
[31] W. Jia, G. Wilar, I. Kawahata, et al., Impaired acquisition of nicotine-induced conditioned place preference in fatty acid-binding protein 3 null mice, Mol. Neurobiol. 58 (5) (2021) 2030–2045, https://doi.org/10.1007/s12035-020-02228-2.
[32] M.H. Wang, Z.L. Chen, L. Yang, et al., Sappanone A protects against inflammation, oxidative stress and apoptosis in cerebral ischemia-reperfusion injury by alleviating endoplasmic reticulum stress, Inflammation 44 (3) (2021) 934–945, https://doi.org/10.1007/s10753-020-01388-6.
[33] J. Karch, J.Q. Kwong, A.R. Burr, et al., Bax and Bak function as the outer membrane component of the mitochondrial permeability pore in regulating necrotic cell death in mice, Elife 2 (2013), https://doi.org/10.7554/eLife.00772.
[34] U. Anilkumar, J.H.M. Prehn, Anti-apoptotic BCL-2 family proteins in acute neural injury, Front. Cell. Neurosci. 8 (2014), https://doi.org/10.3389/fncel.2014.00281.
[35] L.F. Zhuang, C.N. Li, Q.J. Chen, et al., Fatty acid-binding protein 3 contributes to ischemic heart injury by regulating cardiac myocyte apoptosis and MAPK pathways, Am. J. Physiol. Heart C 316 (5) (2019) H971–H984, https://doi.org/10.1152/ajpheart.00360.2018.
[36] D. Ma, M. Zhang, Y. Mori, et al., Cellular localization of epidermal-type and brain-type fatty acid-binding proteins in adult hippocampus and their response to cerebral ischemia, Hippocampus 20 (7) (2010) 811–819, https://doi.org/10.1002/hipo.20682.
[37] H. Oizumi, K. Yamasaki, H. Suzuki, et al., Fatty acid-binding protein 3 expression in the brain and skin in human synucleinopathies, Front. Aging Neurosci. 13 (2021), 648982, https://doi.org/10.3389/fnagi.2021.648982.
[38] G.X. Song, Y.H. Shen, Y.Q. Liu, et al., Overexpression of FABP3 promotes apoptosis through inducing mitochondrial impairment in embryonic cancer cells, J. Cell. Biochem. 113 (12) (2012) 3701–3708, https://doi.org/10.1002/jcb.24243.
[39] I. Kawahata, L. Bousset, R. Melki, et al., Fatty acid-binding protein 3 is critical for alpha-synuclein uptake and MPP+-Induced mitochondrial dysfunction in cultured dopaminergic neurons, Int. J. Mol. Sci. 20 (21) (2019), https://doi.org/10.3390/ijms20215358.
[40] A. Cheng, I. Kawahata, K. Fukunaga, Fatty acid binding protein 5 mediates cell death by psychosine exposure through mitochondrial macropores formation in oligodendrocytes, Biomedicines 8 (12) (2020), https://doi.org/10.3390/biomedicines8120635.
[41] C.M. Duffy, H. Xu, J.P. Nixon, et al., Identification of a fatty acid binding protein4-UCP2 axis regulating microglial mediated neuroinflammation, Mol. Cell. Neurosci. 80 (2017) 52–57, https://doi.org/10.1016/j.mcn.2017.02.004.
[42] X. Zhou, S. Zhou, J. Tao, et al., HIV-1 Tat drives the Fabp4/NF-kappaB feedback loop in microglia to mediate inflammatory response and neuronal apoptosis, J. Neurovirol. (2022), https://doi.org/10.1007/s13365-022-01094-z, 10.1007/s13365-022-01094-z.
[43] Q. Gao, A. Sarkar, Y.Z. Chen, et al., Overexpression of heart-type fatty acid binding protein enhances fatty acid-induced podocyte injury, Exp. Ther. Med. 15 (2) (2018) 2054–2061, https://doi.org/10.3892/etm.2017.5643.
[44] J. Zhang, B. Sun, J. Yang, et al., Comparison of the effect of rotenone and 1methyl4phenyl1,2,3,6tetrahydropyridine on inducing chronic Parkinson's disease in mouse models, Mol. Med. Rep. 25 (3) (2022), https://doi.org/10.3892/mmr.2022.12607.
[45] X.S. Zeng, W.S. Geng, J.J. Jia, Neurotoxin-induced animal models of Parkinson disease: pathogenic mechanism and assessment, ASN Neuro. 10 (2018), 1759091418777438, https://doi.org/10.1177/1759091418777438.
[46] reply 142-3 J.T. Greenamyre, J.R. Cannon, R. Drolet, et al., Lessons from the rotenone model of Parkinson's disease, Trends Pharmacol. Sci. 31 (4) (2010) 141–142, https://doi.org/10.1016/j.tips.2009.12.006.
[47] J.R. Cannon, V. Tapias, H.M. Na, et al., A highly reproducible rotenone model of Parkinson's disease, Neurobiol. Dis. 34 (2) (2009) 279–290, https://doi.org/10.1016/j.nbd.2009.01.016.
[48] H. Xicoy, B. Wieringa, G.J. Martens, The SH-SY5Y cell line in Parkinson's disease research: a systematic review, Mol. Neurodegener. 12 (1) (2017) 10, https://doi.org/10.1186/s13024-017-0149-0.
[49] P. Li, H. Lv, B. Zhang, et al., Growth differentiation factor 15 protects SH-SY5Y cells from rotenone-induced toxicity by suppressing mitochondrial apoptosis, Front. Aging Neurosci. 14 (2022), 869558, https://doi.org/10.3389/fnagi.2022.869558.
[50] I. Chung, H.A. Park, J. Kang, et al., Author Correction: neuroprotective effects of ATPase inhibitory factor 1 preventing mitochondrial dysfunction in Parkinson's disease, Sci. Rep. 12 (1) (2022) 5203, https://doi.org/10.1038/s41598-022-09076-1.
[51] S.W. Perry, J.P. Norman, J. Barbieri, et al., Mitochondrial membrane potential probes and the proton gradient: a practical usage guide, Biotechniques 50 (2) (2011) 98–115, https://doi.org/10.2144/000113610.
[52] D.G. Nicholls, Fluorescence measurement of mitochondrial membrane potential changes in cultured cells, Methods Mol. Biol. 1782 (2018) 121–135, https://doi.org/10.1007/978-1-4939-7831-1_7.
[53] S. Miwa, S. Kashyap, E. Chini, et al., Mitochondrial dysfunction in cell senescence and aging, J. Clin. Invest. 132 (13) (2022), https://doi.org/10.1172/JCI158447.
[54] M. Jelinek, M. Jurajda, K. Duris, Oxidative stress in the brain: basic concepts and treatment strategies in stroke, Antioxidants 10 (12) (2021), https://doi.org/10.3390/antiox10121886.
[55] M.U. Huun, H.T. Garberg, J. Escobar, et al., DHA reduces oxidative stress following hypoxia-ischemia in newborn piglets: a study of lipid peroxidation products in urine and plasma, J. Perinat. Med. 46 (2) (2018) 209–217, https://doi.org/10.1515/jpm-2016-0334.
[56] H.Q. Zhong, H.Y. Yin, Role of lipid peroxidation derived 4-hydroxynonenal (4-HNE) in cancer: focusing on mitochondria, Redox Biol. 4 (2015) 193–199, https://doi.org/10.1016/j.redox.2014.12.011.
[57] P.E. Czabotar, G. Lessene, A. Strasser, et al., Control of apoptosis by the BCL-2 protein family: implications for physiology and therapy, Nat. Rev. Mol. Cell Biol. 15 (1) (2014) 49–63, https://doi.org/10.1038/nrm3722.
[58] M.S. Ola, M. Nawaz, H. Ahsan, Role of Bcl-2 family proteins and caspases in the regulation of apoptosis, Mol. Cell. Biochem. 351 (1–2) (2011) 41–58, https://doi.org/10.1007/s11010-010-0709-x.
[59] C. Hetz, P.A. Vitte, A. Bombrun, et al., Bax channel inhibitors prevent mitochondrion-mediated apoptosis and protect neurons in a model of global brain ischemia (vol 280, pg 42960, 2005), J. Biol. Chem. 287 (53) (2012), https://doi.org/10.1074/jbc.A112.505843, 44108-44108.
[60] A. Cheng, W.B. Jia, I. Kawahata, et al., A novel fatty acid-binding protein 5 and 7 inhibitor ameliorates oligodendrocyte injury in multiple sclerosis mouse models, EBioMedicine 72 (2021), https://doi.org/10.1016/j.ebiom.2021.103582.